In situ single asperity wear at the nanometre scale

Y. Liao[1] and L. Marks[*2]

The interface of two contacting materials experiences complex physical and possibly chemical reactions when one slides with respect to another. While tribology, a subject studying sliding contact, has been comprehensively elucidated for a variety of materials ranging from metals, carbides, inorganic materials and polymers, direct imaging data of the processes taken place at the nanometre or atomic scale have been greatly lacking. Recent proliferation of precise manipulation of a scanning nano-probe has provided a great tool to image sliding of single asperities, and single asperity nanotribology has been a rapidly developing area which provides model systems to investigate the fundamentals of sliding contacts and surface science. By implementing a nanoprobe in a higher resolution transmission electron microscope or a scanning electron microscope, the materials deformation of sliding single asperities have been revealed in real time, leading to insightful understandings of wear and friction. This article reviews recent reports on *in situ* transmission electron microscopy tribological investigations with an emphasis on materials degradation in mechanical and tribochemical reactions at the nanometre scale and at the surface.

Keywords: Tribology, Wear, Friction, *In situ* TEM, Single asperity

Introduction

How to provide sufficient energy to maintain and improve the quality of life in the developing countries as well as the ever increasing needs of developed countries, while avoiding undesirable consequences such as global warming is one of the critical scientific challenges of the twenty-first century. To quote Samuel Bodman, U.S. Secretary of Energy[1]

> … the largest source of immediately-available "new" energy is the energy that we waste every day.

One of the most pervasive wastes of energy is friction, by some estimates between 2[2] and 6%[3] of the GDP of developed countries. In passenger cars, one-third of the fuel energy is used to overcome friction in the engine, transmission, tyres and brakes.[4] Similar to the potential savings due to reduction in the thermal losses of buildings or improving the efficiency of light sources, reducing frictional losses would go a long way to mitigate the looming energy crisis.

While friction has been appreciated as of critical importance dating back at least as far as the ancient Egyptians, for instance the carving on the tomb of Saqqara 2400 BC showing a man pouring a lubricating liquid to help move a statue of Ti,[5] in many respects our current understanding of tribology, (introduced in the Jost report[6] from the Greek word, 'tribos', meaning 'rubbing' or 'to rub') which includes the sources of friction as well as wear and chemical changes associated with sliding is comparatively limited. It is widely recognised that tribology is a multiscale problem, similar to designing better steels. This means that we need to understand the fundamental materials science relationship between structure and properties at all size scales, ranging from atomic through nanoscale to the micro and macro scales, and it is only when we have this information that it will become possible to make revolutionary rather than incremental improvements.

Wear of tribological components accounts for the costly breakdown and maintenance of applications ranging from orthopaedic implants to automotive engines. Volume loss of sliding contacts is a complicated process depending on both materials intrinsic properties, notably hardness and fracture toughness and extrinsic factors such as contact geometry and environment.[7,8] Tribological studies of two surfaces sliding against each other usually place an emphasis on friction coefficient and wear. At the macroscopic scale, plasticity of the materials, stress distribution, along with environment and sliding speed, have been intensively investigated using conventional experimental techniques and fruitful results have been achieved in the past research.[5,7–9] It is known that macroscopic wear can be induced by different modes such as abrasive, adhesive, fatigue, fretting, erosive and corrosive wear, resulting in different degrees of volume loss.[10–12] From the mechanical perspective, the Archard

[1]Dow Chemical, Performance Silicone, Midland, MI 48686
[2]Department of Materials Science and Engineering, Northwestern University, Evanston, IL, USA

*Corresponding author, email l-marks@northwestern.edu

wear model[13] has been widely proven for general tribological systems that total wear volume loss is proportional to the normal load, the sliding distance and inversely proportional to material hardness. The stresses at the surface are calculated using contact mechanics such as Hertzian contact theory and adhesion.[14–17] In addition to mechanical wear, chemical reactions at sliding contact surface are also important and in many cases critically influence the environment sensitivity.[18–35]

Unravelling wear and other tribological behaviour such as friction and wear require comprehensive understanding of the contacting interface, microstructure and chemistry at the nanometre scale. Owing to roughness, contacting surfaces are composed of numerous small asperities ranging from micro- to nano-meter scale. Bowden *et al.*[17] showed that contact in general only occurs at the apex of local asperity. Macroscopic scale wear, friction and adhesion are primarily determined by the collective mechanical behaviour and/or intimacy of these points of contact.[17,36–38] In microelectromechanical system (MEMS) and NEMS devices micro-meter or nano-metre sized single asperity contact often exhibits high friction and wear.[11,39,40] Compared to the macroscopic wear, knowledge of these individual asperities at the nanoscale are limited,[41] and understanding how they degrade pertaining to sliding processes is essential to design tribological systems. Conventional tribological and wear tests such as pin-on-disc and reciprocating sliding tests measure friction and wear rates at the macroscopic and microscopic scale, and usually do not provide information on the structure evolution in real time.

With recent progress in scanning probe manipulation and force measurement, the information of sliding single asperities become accessible at the nanometre and even molecular level. Extensive work has been reported addressing friction, adhesion and wear of a single asperity using atomic force microscopy (AFM) or scanning tunnelling microscopy (STM).[11,31,42–57] In the past decade, by integrating a scanning probe, which is conventionally used for STM or AFM, into a transmission electron microscope, the evolution of materials structure can be directly imaged *in situ* during sliding. This review overviews recent reports of nano-scale wear of single asperities using *in situ* TEM techniques, with particular interest in the materials evolution at the surface and subsurface. Metals, carbides and diamond-like carbon (DLC) coatings that are widely used in varied tribological systems are included for discussion.

The structure of this review is as follows. The Sections 'Microscopic wear and *in situ* scanning electron microscope' and '*In situ* TEM sliding techniques' overview microscopic wear and the techniques of single-probe wear *in situ* in an electron microscope. The Section 'Wear and tribofilm transfer of layered structure' summarises *in situ* wear of layered 2-D structure such as graphite and MoS₂. The Sections 'Wear of metallic materials', 'Atomistic wear assisted by stress', 'Layer-by-layer wear and dislocation mediation' and 'Tribochemical reactions: ageing, graphitization, and etching' focus on *in situ* wear of inorganic materials, e.g. metals and ceramics. The Section 'Liquid-like behaviors' addresses single-probe wear under controlled environments. The Section 'What do we know, what do not we know, whither the science'0 describes liquid-like behaviour of gold film in nano-scale

sliding contact, followed by remarks on limitations and future of *in situ* tribology in a TEM.

Microscopic wear and *in situ* scanning electron microscope

Wear is material loss from contacting surfaces in relative motion. Wear and friction are related to rupturing the bonding of surface atoms, although a general, simple correlation does not exist. The fundamentals of sliding surfaces were unclear until the surface material properties and interaction could be quantified in the past century.[5] A number of wear mechanisms have been identified both macroscopically and microscopically, such as adhesive wear, abrasive wear, corrosive wear, erosive wear, fretting wear and fatigue wear.[58] In the Archard wear criterion,[59] the real area of contact is determined by the normal stress and material hardness. The initial deformation of a sliding contact is elastic, and the deformation evolves to plastic when the elastic limit is exceeded.

Sliding contact may lead to large plastic deformation in the surface and sub-surface material. It is generally agreed that in metallic and ceramic materials, the plastic shear strain at the surface could be over 10, decreasing rapidly into the subsurface.[41,60] As evident by a number of TEM observations of worn surface, the large plastic deformation is mediated by dislocations even for brittle materials in their bulk form.[61–63] For instance, in their cross-section TEM study of silicon single crystal (111) or (001) surface, Puttick *et al.*[64] observed dislocations generated 100–400 nm beneath the surface. The dislocations are either dislocations loops or dislocation arrays.[64] The deformation can penetrate into tens of microns in abrasive wear as shown in the microscopic work by Sticker and Brooker.[63] The dislocations and dislocation arrays commonly further evolve into dislocation cell structure. The large strain also result in nanocrystalline structure at the surface typically ranging from 10 to 50 nm through either fracture or dislocation cell formation.[65]

Different materials degradation mechanisms such as adhesion, delamination and fatigue, are considered in wear models.[41,66–72] However, sliding interface is complicated by very high local stress distribution, chemical reaction, materials transfer and wear debris as third body. These factors are complex in nature and interrelated.

Micro or even nanometre scale sliding has long been recognised as fundamental to wear and friction. A thorough understanding of the underlying mechanism of nanoscale single asperity wear requires well-defined contact geometries. Gane's[73] pioneering work on indentation in 1970 on gold specimens in a scanning electron microscope (SEM) demonstrated that materials deformation at the nanoscale can be very different from that in the bulk form. Since then researchers have employed electron microscopes to observe real-time micro-probes in sliding contact. In the 1980s, Kato *et al.* implemented a tribometer with a probe sliding on a disc in an SEM to record single asperity wear in real time.[74] Hokkirigawa *et al.*[75,76] reported wear apparatus with a pin on flat miniature system implemented in an SEM. The load could be either a dead weight as shown in Fig. 1*a*, or applied by spring coils.[77–79] *In situ* SEM sliding systems are versatile for a wide variety of materials such as metals and
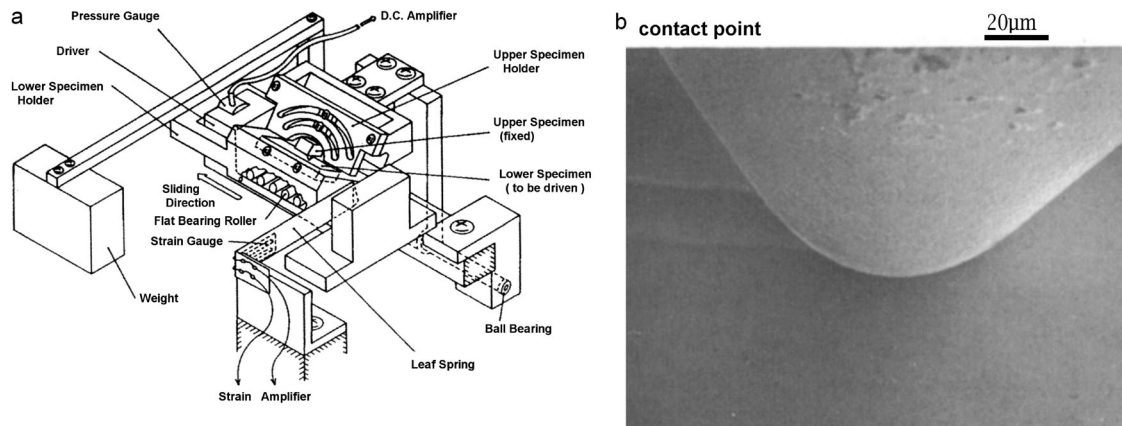
1 *a* A schematic of a tribometer implemented in an SEM.[75] The applied load is exerted using dead weight. *b* SEM micrograph of the wear track and sliding tip[75]

diamond, and the typical size of the asperity and thus the wear tracks were about 20 μm. The sliding speed is typically tens of micro-meter per second. Figure 1*b* shows grooves in a flat bearing steel specimen trailed by a diamond pin under a normal load of <0.5 N. Other than the ridge built on the side, there were no distinct wear particles. Under a higher load of 0.5–1.5 N, a wedge was produced in front of the sliding pin. With increasing sliding cycles, thin plate-like wear debris, i.e. shear tongue, was formed presumably from the wedge.[77] Upon increasing the load to ∼2 N, the pin cut the surface abruptly into long wear particle.[77] The degree of penetration was dependent on not only the hardness, but also the angle between the surfaces. Different wear modes were microscopically recorded in these repeating sliding experiments and are well related to the macroscopic wear diagrams[74] developed using continuum theories.

In situ TEM sliding techniques

Although *in situ* SEM studies provide fruitful experimental data on sliding contact, a SEM only images the surface and often only at relatively low resolution. The time resolution of *in situ* SEM study is limited by the scanning speed of electron beam and a higher scanning speed is usually only possible at the cost of spatial resolution. The magnitude of the motion distance as well as the size of the mechanical probe in a typical *in situ* SEM wear test is ∼20 μm, while the surface roughness of a polished metal surface is usually in the tens of nanometres to sub-micrometer size range. A smaller tribological system and higher resolution imaging techniques are essential for examining wear at the nano-meter scale.

TEM is a powerful tool for probing smaller features. Compared to SEM, TEM can resolve features of nanometre to angstroms size in routine use. A TEM image is formed using a parallel beam so is a full-frame image, thus time resolution is primarily limited by the sampling rate of the camera. For electron imaging and spectroscopy theories of TEM, the readers are referred to the books in references[80–84] for details. TEM probes structure change not only at the surface, but also in the sub-surface as high-energy electrons travel through a very thin material, providing extremely desired information for tribological studies. Combined with electron dispersive spectroscopy

(EDS), electron energy loss spectroscopy (EELS) and diffraction techniques TEM enables local structural and chemical analysis in real time.

The first *in situ* contact micro/nanoprobe in an SEM and/or TEM dates back to 1968–1970 when Gane[75] and Gane and Bowden[37,73] designed a contact probe for an AEI Scientific Instrument E.M. 6 TEM. Gane and Bowden[37,73] exploited a piezo-bimorph actuator, as shown in Fig. 2*a*, to apply load from 2 μN to 10 mN, and a silicone oil dashpot to dampen the mechanical vibration amplitude to around 5 nm. The development of *in situ* TEM techniques for tribology, however, was sporadic until late 1980s when Spence *et al.*[54,88–90] incorporated a scanning tunnelling probe within a TEM which enabled simultaneous high-resolution observation of moving objects in transmission mode. This major progresses were soon followed by other groups with various design of side-entry TEM holder implemented with scanning probe or atomic force tips.[91–98] A variety of *in situ* nanoindentation tests were also designed with high-stiffness indenter and accurate normal force measurement.[98,99] Tokushi *et al.* implemented STM type tips in time-resolved HREM, and successfully demonstrated the one atomic layer removal during a sliding event.[100] The authors[100] observed stick-slip motion in gold–gold sliding system and attributed the stick-slip to the formation of grain boundary at the surface.

In the past decade, commercial TEM holders manufactured by Hysitron, Nanofactory and others have enabled *in situ* tribological experiments for various material combinations at higher resolutions and precision. Figure 2*b* and *c* shows commercial *in situ* nanoindentation/tribology TEM holders using a diamond tip and tungsten probe, respectively. In the STM-TEM tribological system shown in Fig. 2*c*, the test specimen is held in a 3 mm TEM grid and mounted 30° to the horizontal direction. The sliding single asperity is capable of both coarse and precise motion in three dimensions. The step resolution, when the motioned motion is driven by a piezo-motor, is typically 0.2 Å in XY and 0.025 Å in Z. The normal load is usually measured by a spring system or by displacement in TEM images based on the known spring constant of an AFM cantilever. In the cases where the normal force cannot be directly measured, the contact pressure can be calculated from the geometry of the
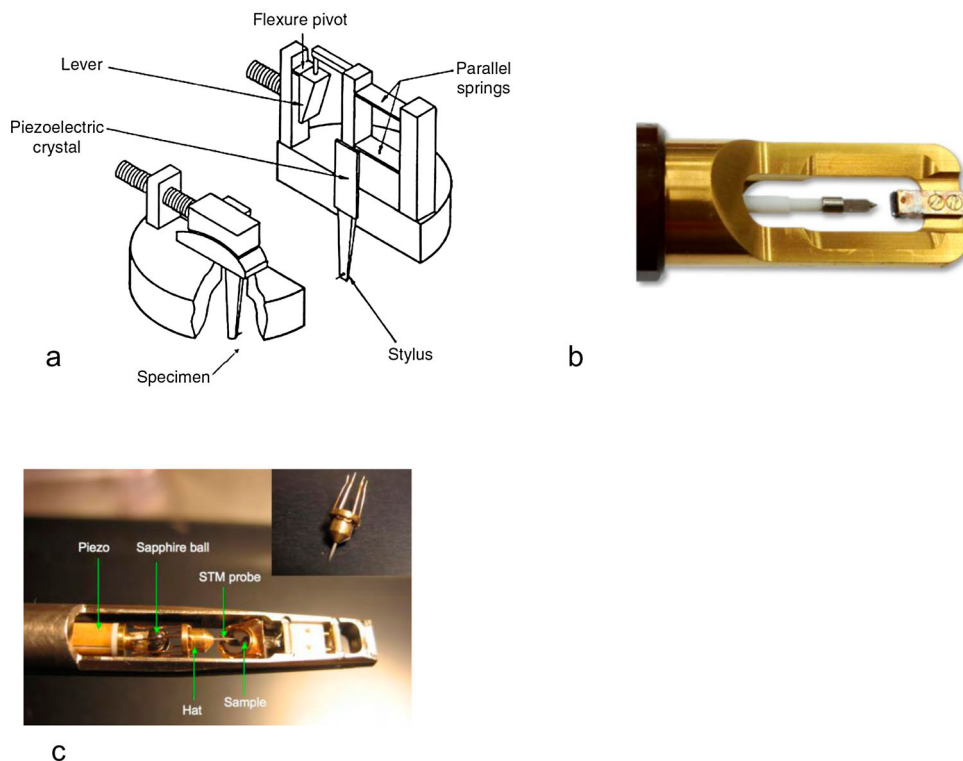
2 *a* The first *in situ* TEM sliding apparatus driven by a piezo-bimorph actuator.[37,73] The stylus must have been attached to the column. *b* The *in situ* TEM holder designed by Hysitron.[85] A diamond tip is attached to a transducer and piezo-electric actuator. *c* An STM-TEM tribological system. The sample is inclined ~30° to enable real-time imaging of sliding events. The inset shows the hat fixture with gripping arms[86,87]

contact using classic contact mechanics. Nafari *et al.*[101] designed an AFM sensor system for *in situ* TEM holder which implemented a Wheatstone bridge circuit using standard micromaching techniques to measure normal force. A reference cantilever was fabricated as one of the bridge resistors to compensate temperature fluctuation. The electrons are conducted through the substrate to one of the connection pads. With careful fabrication, the noise level of this sensor is reported to be ~15 nN. The MEMS-sensor is $1.2 \times 1.3 \times 0.5$ mm^3, enable ~30° tilt in the pole piece of a TEM. The holder can also measure normal force using the resistance change. Sato *et al.*[102] designed a MEMS in which two opposing tips driven by electrostatic actuators can achieve both lateral and longitudinal motion with reduced vibration. In an Ag–Ag sliding test the authors observed stepwise motion similar to the atomic resolution.[102] Although force measurement in 3D, particularly in the lateral direction is still elusive, the existing *in situ* TEM tribological techniques have significantly deepened our capabilities of collecting nano-scale wear imaging data in the real time.

In situ TEM samples require electron-transparency and can be prepared by multiple methods such as thin films deposition,[103,104] argon ion beam cutting,[100] focus ion beam (FIB) thinning,[105] MEMS fabrication[102] and mechanical transferring of layered structures.[106] It is worth emphasising that harsh sample preparation can introduce defects and/or impurities prior to the tribological tests.[107] Caution is needed in the processing of aligning the counter parts as the axis of the probe does not always align with the tilt axis of the TEM. Motion in either *X* or *Y* direction commonly yields displacement in the Z direction. In practice it is useful to align both the tip and testing specimen to the eucentric height by minimising the magnitude of wobbling.

Interpreting a TEM image involves a thorough understanding of electron interaction with matter, which is not simple in many cases. Current *in situ* TEM tribological tests mainly depend on mass contrast of single phase materials. This contrast is sufficient to identify the morphology and wear volume when care is taken. Owing to the limitation of single-tilt holder and small pole piece gaps, the sample is usually positioned off well-defined diffraction condition (such as two-beam condition or low-index zone axis), making diffraction contrast and high-resolution phase contrast analysis extremely difficult. Additionally, sample vibration during a sliding test results in large focal spread and further limits the resolution of materials in sliding. With the assistance of development of damping system,[20,108] high-resolution images are usually obtained during the interval between sliding tests when the sample is stationary. High speed cameras, double tilt capabilities and better imaging processing techniques are desirable for understanding structural and chemical change at the atomic scale.

Most *in situ* TEM sliding tests are performed in vacuum with reciprocating sliding at very slow speed, typically a few hundred nanometres per second. Thus the frictional heating is minimal for metals and other heat-conductive materials. With advanced environment cells,[109] sliding tests in controlled environment can be done. Electron beam damage and contamination can be important, especially for beam sensitive materials such as hydrocarbon materials. Excessive exposure to the
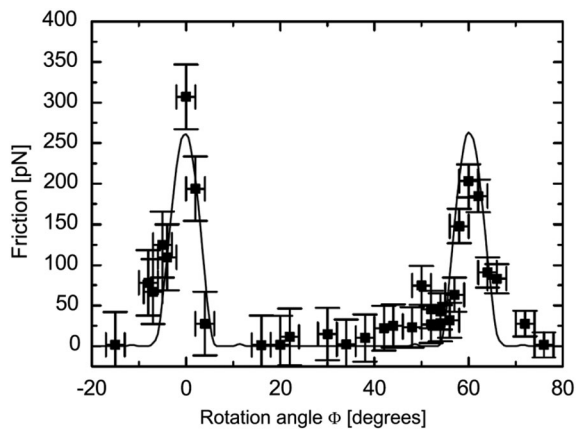
3 Friction of graphite as a function of rotation angle. High friction peaks were present at 0° and 61° corresponding to aligned interfacial lattice. Superlubricity occurred at intermediate angles due to incommensurate contact surfaces[122]

electron beam should be avoided by reducing the exposure time and/or using a small condense aperture.

## Wear and tribofilm transfer of layered structure

Layered structures such as graphitic materials and molybdenum disulphide are some of the most important solid lubricants and have attracted substantial research interest to understand their sliding behaviour. As one of the allotropes of carbon, graphite is composed of hexagonal sheets where the carbon atoms are covalently bonded in plane. Graphite has been widely used for lubricants [47,110–120] as the interlayers bonded by weak van der Waals force and can readily slide. In AFM or frictional force microscopy (FFM) experiments, atomic scale single asperities showed extremely low friction coefficient of 0.001 when sliding on graphite or MoS_2.[117,121] These asperities often experience periodic, discontinuous movement, i.e. stick-slip. Dienwiebel *et al.*[122] developed an FFM with ultra-high lateral force resolution as precise as 15 pN, and slid a silicon tip again a highly ordered pyrolytic graphite (HOPG) specimen at different angles. As shown in Fig. 3, friction force peaks were recorded to be $61 \pm 2°$ apart, corresponding to the 60° rotation

symmetry. The friction dropped to nearly zero friction force for the intermediate angles showing evidence of incommensurate interfacial sliding. The authors suggested that a graphite flake had been transferred to the tip. When the flake was crystallographically aligned to the substrate the friction peak occurred. The dynamic process of tribofilm transfer, however, remained largely unknown.

Merkle and Marks[106] rubbed a tungsten probe on HOPG flakes using an *in situ* STM-TEM holder. HREM images after 100 passes show clear evidence of 5–35 layers of ordered graphic basal planes with defects in the wear track in the HOPG. Closer inspect of the tungsten counterpart indicated that graphite layer transfer had taken place. Figure 4a[106] shows the HREM image of the tungsten tip surface where a ~2.5-nm thick graphite flake was present. This is a direct imaging of graphite transfer film in real time, confirming the prediction that a graphite–graphite contact can be established during sliding and thus provides highly lubricious interface.[122]

In a recent report by Casillas *et al.* graphite flakes sliding against silicon was examined using an AFM-TEM holder and a JEOL 2010F TEM.[123] HOPG flakes were attached to a 0.5-mm gold wire by repeated peeling similar to the way of obtaining graphene. The normal pressure was calculated based on the displacement of the cantilever and the tip size to be 150–500 MPa. Figure 4b shows typical time sequences of sliding on graphite, in which a single layer of graphite was transferred to the silicon tip. The top layer of graphite was deformed and frequently buckled ~3 nm, equivalent to ~20 atoms, ahead of the sliding tip. These buckles fractured, resulting in small flakes which were subsequently transferred to the silicon tip. Similar single layer transfer was also observed in *in situ* tests on MoS_2, while MoS_2 transferred layers were typically 5–20 nm in size, longer than the small graphitic transfer layers. The difference presumably originated from the bending modulus and strength. Single sheet to graphite can be readily deformed, bent or even crumpled,[124] while the S/Mo/S sandwich structure is bonded by covalence bonds within the layer thus the single layer is more resistant to bending.

A few layers of MoS_2 have also been manipulated by a tungsten nano-probe *in situ* in a TEM using a STM-TEM holder.[125] Oviedo *et al.*[126] reported *in situ* TEM sliding test of a few layers of MoS_2 sheet against a tungsten probe with 6–8 nm native oxide layer. By applying ~10 V bias, nine layers MoS_2 nanoflakes adhered to the
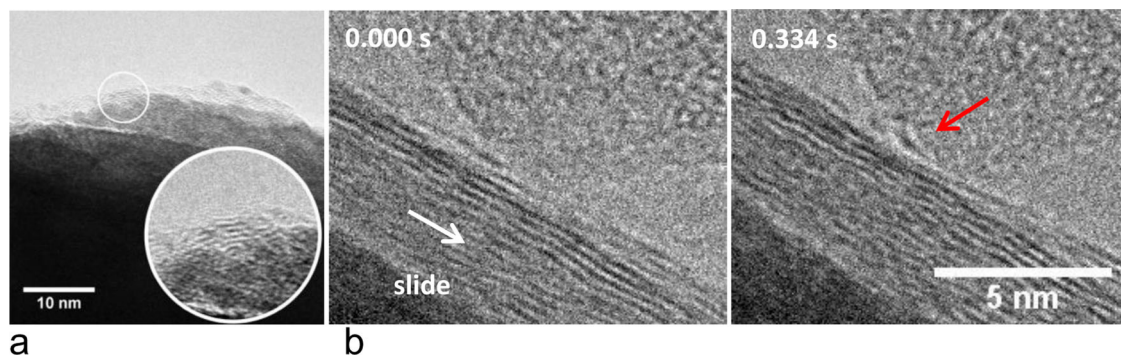
4 *a* Transfer layer in a tungsten probe after 100 passes.[106] The inset shows a few layers of lamellar structure. *b* A series of TEM micrographs showing monolayer graphite sheet was transferred to a silicon AFM tip
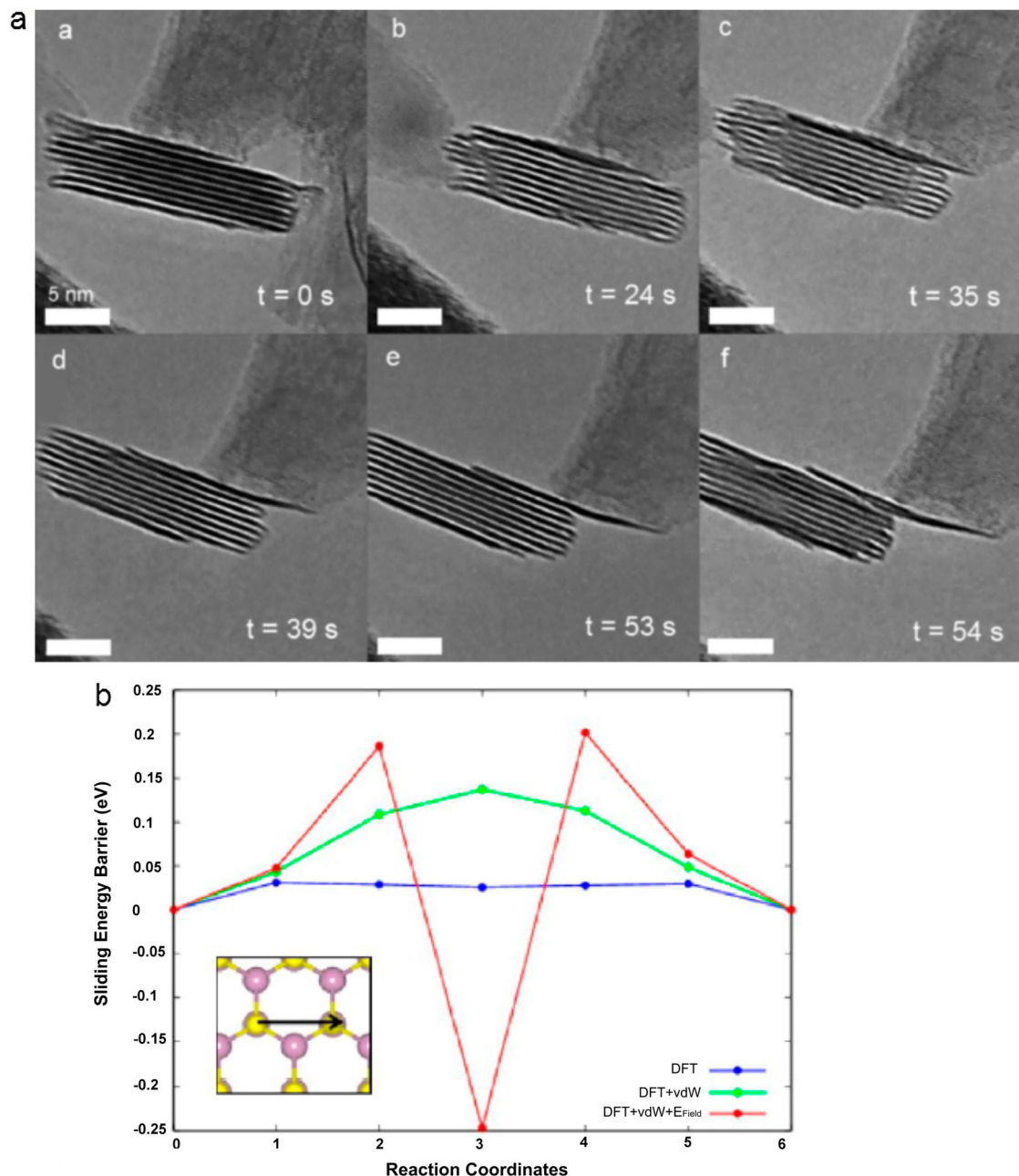
5   *a* A series of TEM micrograph showing monolayer sliding and transfer to the oxidised tungsten tip at a bias of 10 V. *b* The sliding energy in the [100] direction is ∼0.14 eV without external electric field (green line). The red line shows the energy barrier with 5 V/nm bias. The sliding of MoS$_2$ layer experiences a higher initial barrier of 0.2 eV, followed by a negative energy barrier of −0.25 eV[126]

probe driven by a piezo-electric motor. Figure 5a shows that a monolayer of MoS$_2$ was sheared from the MoS$_2$ surface, and subsequently transferred to the tungsten probe. The sliding was then mediated by relative motion between MoS$_2$ sheets. Figure 5b shows energy barriers to sliding a MoS$_2$ layer in [100] direction calculated using density functional theory. The barrier is ∼0.14 eV without an external electric field. The barrier initially increased to ∼0.2 eV with 5 V/nm polarisation, and dropped to −0.25 eV after the first barrier. Oviedo *et al.*[126] measured the shear strength of single layer MoS$_2$ to be 25.3 ± 0.6 MPa in the TEM column with a low vacuum of 2×10^{-5} Pa. This result is consistent with the macroscopic shear strength of 24.8 ± 0.5 MPa

which was determined by Singer *et al.* for sputtered MoS$_2$ films.[127]

Inorganic fullerene (IF) MoS$_2$ and tungsten disulphide (WS$_2$) nanospheres have been extensively studied as friction modifier due to their excellent friction resistance and thermal stability.[116,128–131] The lubricity of these nanoparticles is suggested to originate from exfoliated layers or particle rolling.[130–132] Lahouij *et al.*[133] slid IF-MoS$_2$ nanospheres between a silicon edge and an AFM tip. The AFM tip was truncated using a FIB to ensure large flat contact thus allowing particles to roll between the surfaces. The authors observed that under 100 nN of applied force IF-MoS$_2$ particles agglomerated and rolled between the surfaces. At 400 nN the integrity of the

nanoparticles was damaged and exfoliation started to take over the wear process. Depending on the active mechanism, the crystallinity of IF-MoS$_2$ particle influenced the friction in different ways. A low degree of crystalline is beneficial to friction reduction when exfoliation is active as the exfoliation process is assisted by the defects in the crystalline.[130,132]

The results of *in situ* sliding of layered structures taking place at the atomic scale is consistent with previous post-facto observation at the nanometre scale and microscopic scale.[134] Sliding contact often involves wear particles and material transferred from one surface to the counterface. Godet[135] and Singer *et al.*,[136] among many others, showed the importance of transfer layer in wear and friction, particularly for solid lubricants such as graphite,[137–139] MoS$_2$ [114] and other transition metal dichalcogenides such as WS$_2$ that exhibit excellent lubricity only in dry or vacuum environment. Scharf *et al.*[140] showed in their cross-section TEM examination of a wear track that sliding (>1000 cycles) on amorphous MoS$_2$ resulted in about nine layers of MoS$_2$ sheet (~6 nm thick). *In situ* TEM sliding imaging data showed that the transfer layer is primarily only one single sheet agreeing with the findings of monolayer transfer layer formation by Dunn *et al.*[141]

Wear of metallic materials

Wear of metallic material depends on both the intrinsic materials properties and contact geometry. Cobalt–chromium–molybdenum (CoCrMo) alloys are an important wear and corrosion resistant material which has enjoyed extensive use in medical devices.[142] Some hip replacements made of CoCrMo alloy have served well *in vivo* in the patients' body for over 20 years.[143–146] Although numerous simulator tests have been conducted in the past decade,[23,147,148] the generation of nanoparticles as wear debris during use is not as yet fully understood. As-cast CoCrMo alloy is composed of an fcc metastable matrix and M$_{23}$C$_6$ or M$_6$C carbides.[149–151] In order to obtain direct imaging data of sliding CoCrMo surface, *in situ* sliding tests of the ductile fcc phase of a cast CoCrMo alloy (complying with ASTM standard F75) were attempted,[105] and the wear processes exhibited similar dependence on the contact geometry as observed in micro-meter scale *in situ* SEM wear test. As shown in the serial frames in Fig. 6a, a ductile lamella was in repeated sliding contact with an AFM tip.[105] The normal pressure was 144–230 MPa. The silicon tip was kept intact throughout the test, and wear primarily occurred in the fcc phase. In the occasions when the fcc phase slid toward the right hand direction, surface cracks were formed chipping off small pieces of materials, with volume ranging from ~3.7 × 10^5 nm^3 to ~1.2 × 10^6 nm^3. The attacking angle between the tip and surface was 64°. The degradation mechanism switched to ploughing when the fcc phase slid toward the left direction at an attack angle of 24°. The silicon tip penetrated into the surface by ~52 nm. After sliding ~1160 nm, the tip removed
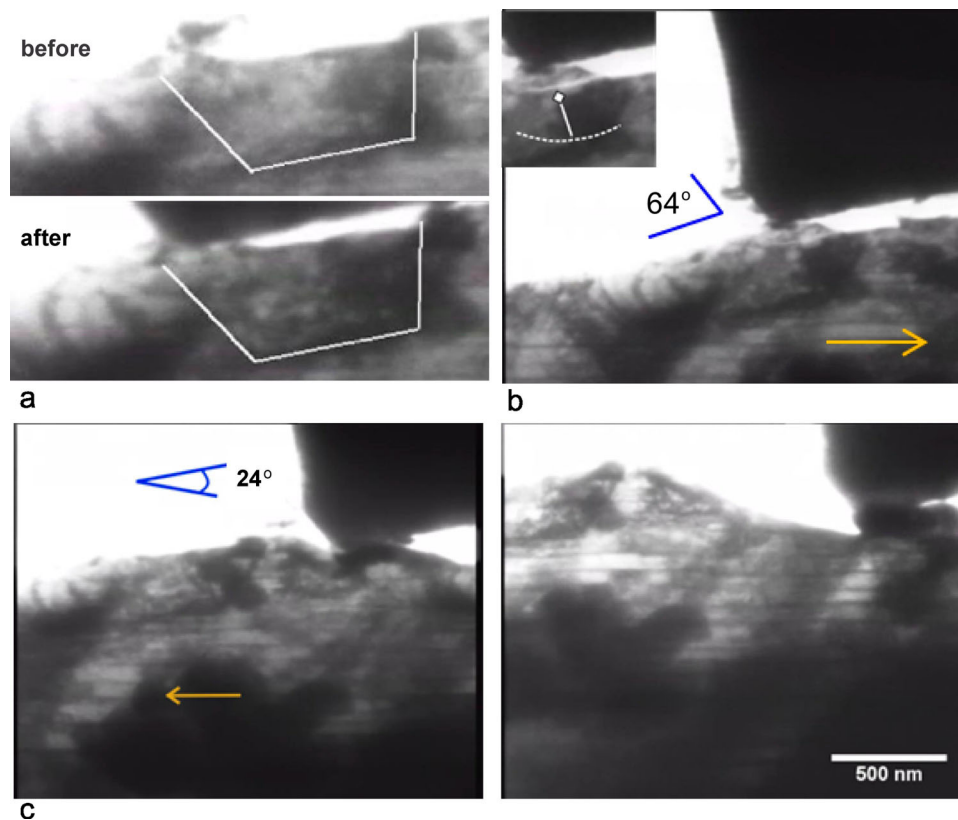
6 *a In situ* **sliding on CoCrMo fcc matrix introduced plastic deformation in the sub-surface.** *b* **A crack was produced when the sample moved to the right-hand side (arrowed). The attack angle was 64°. The zoom-in micrograph in the inset shows curved crack propagation under the contacting point.** *c* **Ploughing dominated at an attack angle of 24°. From reference[105]**

$\sim 3.0 \times 10^6$ nm^3 with the wear volume accumulated in front of the tip in the sliding direction.

The *in situ* sliding of CoCrMo fcc matrix experiment shows that continuum models are still largely valid in nano-scale wear of plastic materials. The wear process exhibits a strong correlation with the geometry of the contact, particularly the attacking angle. This observation of abrasive wear at the nanometre scale is exceedingly similar to the microscopic abrasive wear study reported by Murray *et al.*,[152] Challen *et al.*,[153,154] and Kato and his co-worker.[74,155] Murray *et al.*[152] found that the attack angle for cutting-ploughing transition was 60° for heat-treated 1040 steel (179 HV) and 30° for 1082 steel with higher strength of 858 HV. In their *in situ* SEM sliding tests of plastic materials, abrasive wear switched from ploughing at an attack angle lower than 40° to cutting (chipping) mode at higher attack angles. Challen and Oxley showed that ploughing and cutting mechanisms can be elucidated by the plane-strain slip line field model.[153] A single asperity sliding on a ductile material creates a wave ABCDE as shown in Fig. 7a. The material volume flowing in and out reaches equilibrium as required by continuity. It was demonstrated that a wedge initially dug in the surface forms a plastic wave in front of it and eventually climbs until the wave migrate to the surface.[9,156] Wear is associated with the material hardness (shear strength) as well as the geometric attack angle α. To evaluate the acting wear mechanism, the degree of penetration D_P, a severity index of contact, is used:

$$D_P = \frac{h}{a} = R \left(\frac{\pi H_v}{2W} \right)^{1/2} - \left(\frac{\pi H_v R^2}{2W} - 1 \right)^{1/2}$$

where a is half of the contact width, h the depth of wear scar, H_v hardness of the plastically deformed material, W normal load and R tip radius. The attack angle is related to D_P by[153]

$$D_P = 0.8 \tan\left(\frac{\alpha}{2} \right)$$

Hokkirigawa *et al.*[75] developed a wear diagram based on their *in situ* SEM sliding results. As shown in Fig. 7b, ploughing prevails at lower angles (<30°) for bearing steels. Wear model transits to cutting at ~40° and above. Figure 7c shows similar results reported by Doyle and Samuels[157] that the cutting model is active when the attack angle is >40°. The nano-scale *in situ* TEM wear of ductile CoCrMo fcc phase agrees with the microscopic wear models based on slip-line theory and plastic deformation.

Substantial sub-surface deformation, wear and tribo-film transfer are reported in other *in situ* TEM wear of metallic systems. Anantheshwara *et al.* slid a tungsten probe on an Al–Mg alloy specimen.[158] Defects of 10–30 nm in size were generated under the contacting

a

b

c
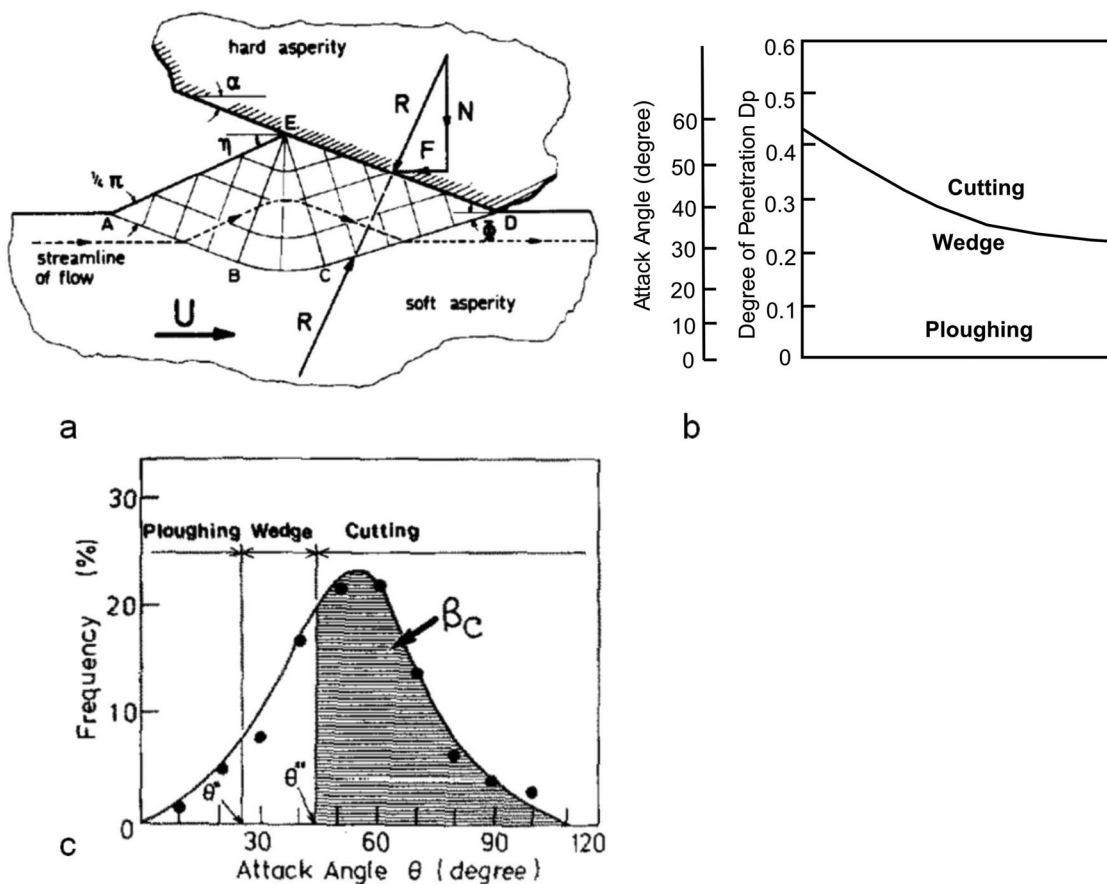
7 *a* Schematic of the slip-line theory showing a wave ABCD in front of a sliding hard asperity.[153] *b* Wear model diagram developed in microscopic wear experiments by Hokkirigawa *et al.*[75] *c* Wear mechanism as a function of attacking angle developed by Doyle and Samuels.[157] Both diagrams show that ploughing is likely to occur at <30°, consistent with the *in situ* TEM sliding experiments at the nanoscale

interface as shown in Fig. 8a, presumably due to sub-grain formation or localised subgrain rotation under high shear strain. The defects further developed into cracks and propagated across the sub-surface. Figure 8b shows the overview of the tungsten tip (the dark region). A thin layer of Al–Mg film was transferred and attached to the tungsten tip in less than one second. The deformation is consistent with a number of post-facto TEM observations of large localised deformation such as dislocations and nanocrystallines in macroscopic repeated sliding.[41,159–161]

Atomistic wear assisted by stress

Jacobs and Carpick[162] reported atomistic wear of silicon through stress-assisted chemical reaction in *in situ* sliding of a silicon AFM tip against a diamond punch. The sliding test featured adhesive force with no applied load. Using trace profiles of four silicon tips, the authors calculated the volume loss at varying intervals. Figure 9a shows the volume lost for four tests as a function of slide distance. The volume lost showed no linear correlation with the product of sliding distance and load (see Fig. 9b), thus the Archard equation[163] is not responsible for the wear. The authors ascribed the wear to a thermally activated process and the kinetics of the wear can be fitted using an Arrhenius equation:

$$\gamma = \gamma_0 \; e^{-(\Delta U_{act}/k_B T)} \; e^{(\sigma \Delta V_{act}/k_B T)}$$

where γ is wear rate, γ_0 a pre-factor, ΔU_{act} the energy barrier to material removal, ΔV_{act} activation volume, $\sigma \Delta V_{act}$ the work done by the stress. Jacobs and Carpick[162] demonstrated an exponential dependence of volume loss on the work done by the adhesive load, as shown in Fig. 9. The normal stress was calculated using the Derjaguin–Muller–Toporov (DMT) model.[29,30] All tests showed that the reaction was more associated with time in contact than the distance slid. Fitting the wear rate data as shown in Fig. 9c using the Arrhenius equation yields an activation volume of 6.7 ± 0.3 Å^3 and energy barrier of 0.91 ± 0.06 eV, which are comparable to the volume of single atom bonding energies.[162] Thus the wear was a stress-assisted chemical reaction and the volume removal was dominated by the kinetics of this chemical reaction. The *in situ* TEM atomistic wear reported by Jacobs and Carpick varied between 500 nm^3 and 4000 nm^3 per micron of sliding.[162,164]

Similar exponential dependence of wear rate on stress has been reported in several nano-scale scanning probe wear tests, most of them involving extremely mild wear of single atom removal.[165–169] Gotsmann and Lantz[165] slid an AFM tip again polymer, and calculated that the volume loss was ~1 atom per micron sliding. Bhaskaran *et al.*[166] observed atomic volume loss of ~1 atom per micron in sliding of DLC coating. Gotsmann and Lantz's wear model[165] suggested that normal pressure had minimal contribution to wear, and that the lateral, frictional force was responsible for the exponential dependence of wear. By fitting the experimental data, Gotsmann and Lantz calculated the effective barrier and activation volume to be 0.983 and 5.5×10^{-29} m^3,[165] respectively.

Layer-by-layer wear and dislocation mediation

Hard engineering ceramic materials have been extensively exploited as wear resistance materials due to their hard nature and resistance to oxidation.[170,171] The degradation of ceramics in sliding contact is frequently attributed to fracture at surface and sub-surface. Liao and Marks[172] reported monolayer-by-monolayer wear of a hard $M_{23}C_6$ carbide phase in CoCrMo alloy. The carbide slid against a flat silicon tip using an AFM-TEM holder under a mild pressure of ~20 MPa, which is significantly lower than the yield strength of the carbide. Figure 10a shows the carbide and the AFM tip before the test. The white lines highlight the carbide geometry after 250 sliding passes. This carbide phase showed steady
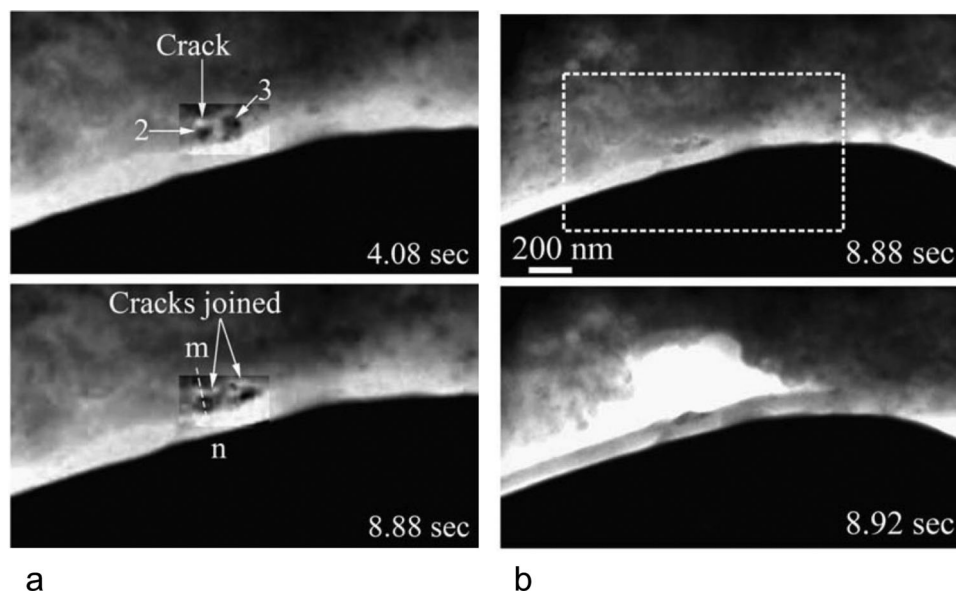

8 *In situ* sliding of a tungsten probe (dark) on an Al–Mg alloy specimen. *a* Serial TEM micrographs showing defects in the contact surface, presumably being subgrain generation or rotation. A crack was developed at the defects. *b* Overview of the tribological system. A transfer layer of Al–Mg was detached and transferred to the tungsten probe[158]
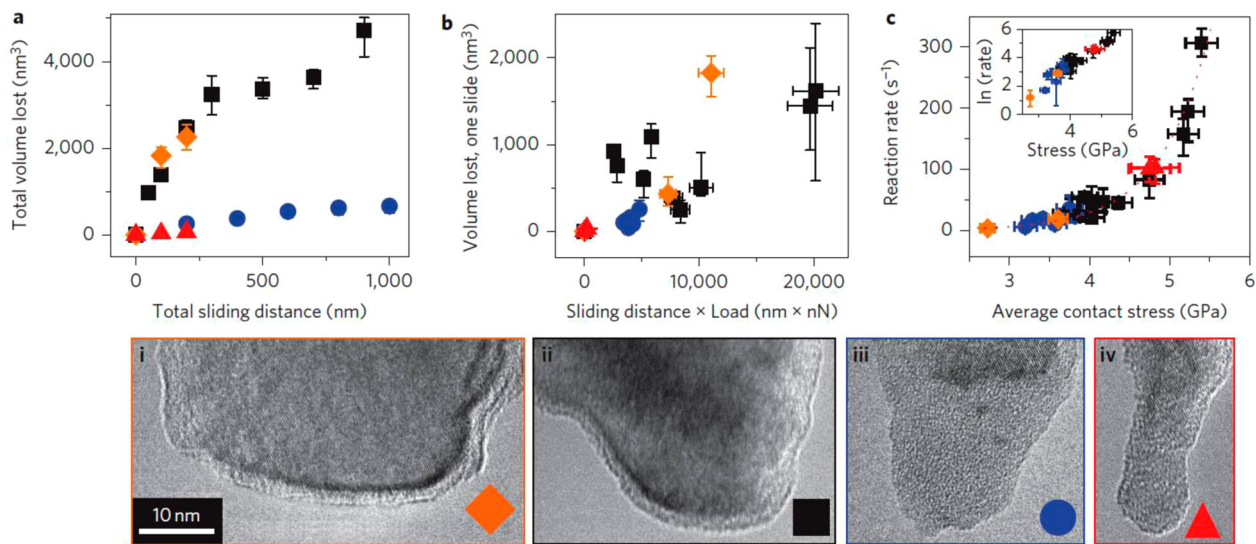
9 **Atomistic wear reported by Jacobs and Carpick. Wear volume in the *in situ* sliding experiments shows exponential dependence on contact stress, indicating the process is stress-assisted thermal activations[164]**

material removal along [511] plane, with no cracks in either the surface or the sub-surface. Figure 10b shows a large number of debris transferred to the silicon tip. As shown in the wear loss as a function of sliding passes in Fig. 10c, the thickness of the carbide was reduced by ∼46 nm over 250 sliding passes, or ∼0.18 nm per pass. This reduction is comparable to the $(51\bar{1})$ planar spacing of 0.20 nm,[173] suggesting that on average, one sliding pass removed approximately one monolayer. The wear coefficient was ∼0.8, indicating that the layer-by-layer wear is a severe wear process. A number of wear debris nanoparticles were generated and transferred to the silicon tip. Figure 10d shows an $M_{23}C_6$ wear debris of ∼8 nm in size. No dislocation was observed in the debris particle due to the small size and brittle nature of the carbide.
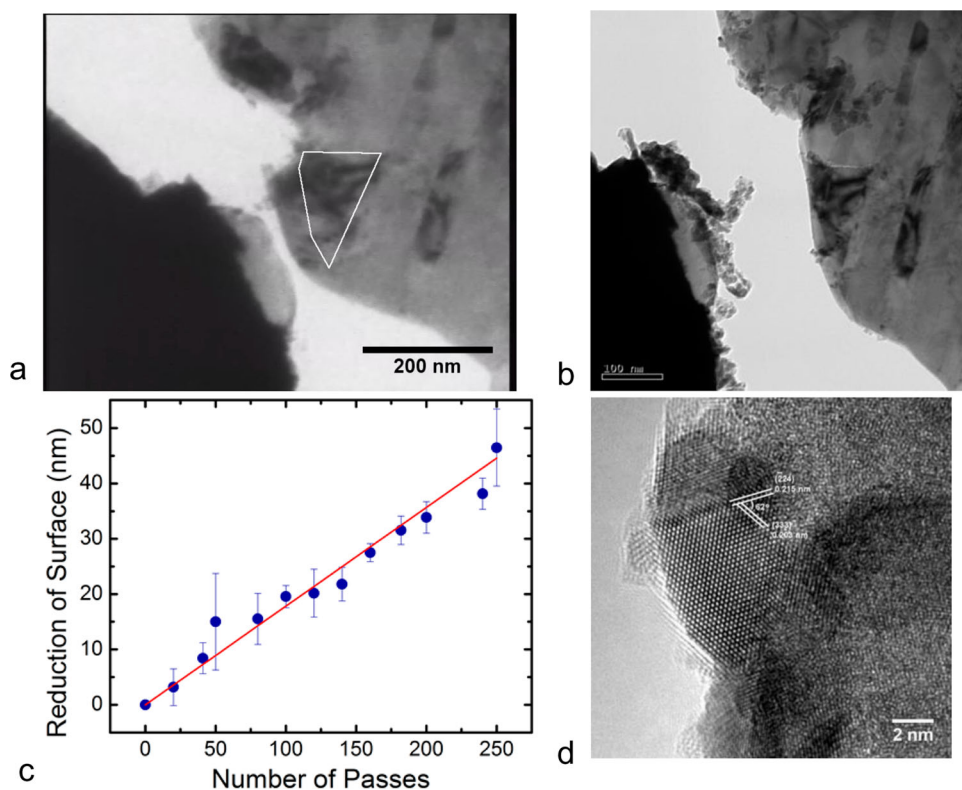
10 **In situ sliding of silicon on an $M_{23}C_6$ carbide. *a* The carbide surface was oriented to [511]. The white lines represent the geometry of the carbide after 250 slide passes. *b* Wear debris were transferred from the carbide base to the silicon tip. The micrograph was taken when the specimen was still. *c* The material removal rate (∼0.18 nm/slide pass) is nearly linear and close to the layer spacing. *d* High-resolution micrograph showing a ∼8 nm debris particle. No dislocations were found in the particle[123]**

The layer-by-layer wear is attributed to shear stress and misfit dislocations residing one layer from the carbide surface, and peel of the surface layer as it moved with the tip.[172] Misfit dislocation exiting at solid–solid contact has been extensively investigated in thin films.[174–178] In the situation where plastic deformation at a sliding interface is mediated by misfit dislocations, the crystallographic structure of the two surfaces plays a critical role.[179,180] Bowden and Tabor[38,181,182] pointed out that the friction force experienced by a single asperity is composed of two components, i.e. the shearing components at the interface (F_D) and the ploughing component in front of the tip (F_p). The plowing force, $F_p = \vartheta \cdot A$, can be considered as a creep process where the relationship between strain rate and shear stress ϑ is[183]

$$\vartheta = A_2 \frac{D_v Gb}{kT} \left(\frac{\sigma_s}{G}\right)^n$$

The shearing component can be modelled by moving a misfit dislocation at the surface.[184] It is a collective contribution of phonon-wind (B_w) flutter effect (B_{fl}) and electronic damping (B_e)

$$F_D = \frac{N_d(\sigma_p b)(\sin\theta + \cos\theta)}{2} \cot\left[\frac{2(\sigma_p b)\sin(\Delta\theta/2)}{B_{tot}v}\right]$$

$$B_{tot}v = B_w + B_{fl} + B_e$$

σ_p is the Peierls stress, B_j the drag coefficients for different effects, v velocity of dislocation, b Burgers vector, N_d the number of dislocations in the contact area, θ the absolute in-plane misorientation angle, $\Delta\theta$ is the angular different from the slip plane. The dragging force is strongly anisotropic. Only dislocation with Burgers vector component in the direction of sliding contributes to dislocation dragging. Misfit dislocations can stand off from the interface at a range of distance from mono-atomic layer to over 20 atomic planes depending on the shear moduli different and lattice registry.[179,180] Materials removal and the transfer layer can be correlated to dislocation stand-off when the sliding is primarily mediated by dislocation motion in the surface.[183,185]

Wear process observed in *in situ* TEM tests varies drastically with the materials and test conditions. For instance, in the atom-by-atom wear of silicon AFM tip, severe wear took place at no applied load and was dominated by thermal activation and adhesion (normal) force.[164] The layer-by-layer wear of $M_{23}C_6$ carbide features steady wear mediated under ~20 MPa. In the report by Ananteshwara *et al.*[186] on sliding tests between a diamond pin and aluminium alloy, the aluminium alloy did not exhibit any wear at contact pressure of 550–900 MPa. Wear began to take place at 1.7 GPa.[186] The initial material removal was ~80 nm in 20 sliding passes, and the wear rate gradually slowed down. After 50 sliding passes the tribological system was stabilised with no further wear recorded. It was observed that wear debris from the aluminium specimen scooped out a chunk of surface material.[186] The wear debris can accumulate and roll between the surfaces. The presence of wear debris remarkably complicates microscopic wear process and deserves further investigation.

Tribochemical reactions: aging, graphitisation and etching

Tribochemical reactions are another critical component in many tribological processes, associated with chemical structure changes which are usually time dependence. It has been observed that sp^3-bonded carbon atoms in DLC film experiences transition into sp^2-boding.[187] Pastewka *et al.*[188] performed MD simulation and suggested that sp^3 carbon bonds in diamond undergo a sp^3-to-sp^2 order–disorder transition upon polishing. This transition is mechanochemically activated, strongly dependent on the anisotropy of diamond crystallographic surface orientation. As shown in Fig. 11, surface carbon atoms leave their crystalline position, building an amorphous layer.[188] The amorphisation featured only one atom at a time, so called 'pilot' atoms. This atomistic process driven by force cannot be fitted with an Eyring-type or Arrhenius-type activation; rather the thickness, h, of the amorphous carbon layer is described by the following equation.[188]

$$h(t) = -\beta + \sqrt{(\beta + h(t_0))^2 + 2(C_{(s1)\langle d1\rangle} P_{(s1)\langle d1\rangle} + C_{(s2)\langle d2\rangle})P_{(s2)\langle d2\rangle})\alpha v_0(t - t_0)}$$

where $C_{(si)\langle di\rangle}$, α, β are constants, t time, $P_{(si)\langle di\rangle}$ the probability for amorphisation of an atom in surface *si* by sliding in direction *di*, v velocity. The probability for amorphisation is negligible ($P < 10^{-6}$) for the {111} surface, while $P = 0.05$ for {110}⟨100⟩ systems, leading to the anisotropic amorphisation rate.[188]

Merkel *et al.*[104] slid a tungsten probe on hydrogenated, wear-resistant DLC film *in situ* in a TEM in vacuum. Figure 12a shows a bright-field TEM image of DLC film after 200 sliding passes. The EELS spectrum of the sliding contact highlighted by the white circle was monitored at intervals during 300 passes as shown in Fig. 12b.[104] The π^* peak, finger print of sp^2 bonding, increased with sliding passes, providing direct evidence of graphitisation induced by sliding. Graphitic transfer layers were present on the tungsten tip and lowered the friction.

Humidity is known to have deleterious effects on the wear resistance of hydrogenated DLC.[30,189–193] M'ndange-Pfupfu *et al.*[109] examined wear of DLC film *in situ* in an environmental TEM in 0.15–1.5 torr of wet nitrogen or hydrogen gas. Sliding in wet N_2 resulted in remarkable wear, as shown in Fig. 12c, with clear wear traces were produced after only 20 sliding passes. The thickness reduction calculated based on the contrast change was determined to be 2×10^5 nm^3. It was suggested that chemically reactive atoms activated by the sliding reacted with either water vapour, chemically absorbed oxygen or hydroxyl species. In contrast, the DLC film was nearly intact after sliding in wet H_2 gas. The wear resistance is ascribed to the passivation of hydrogen of any active carbon radicals. The accelerated wear in wet N_2 provides quantitative nanoscale evidence of tribochemical reaction taken place at a sliding surface, and is consistent with the macro-scale wear resistance of hydrogenated DLC film.[30,189–193]

Liquid-like behaviours

In addition to microstructural and chemical change, friction may alter the surface such that the surface may
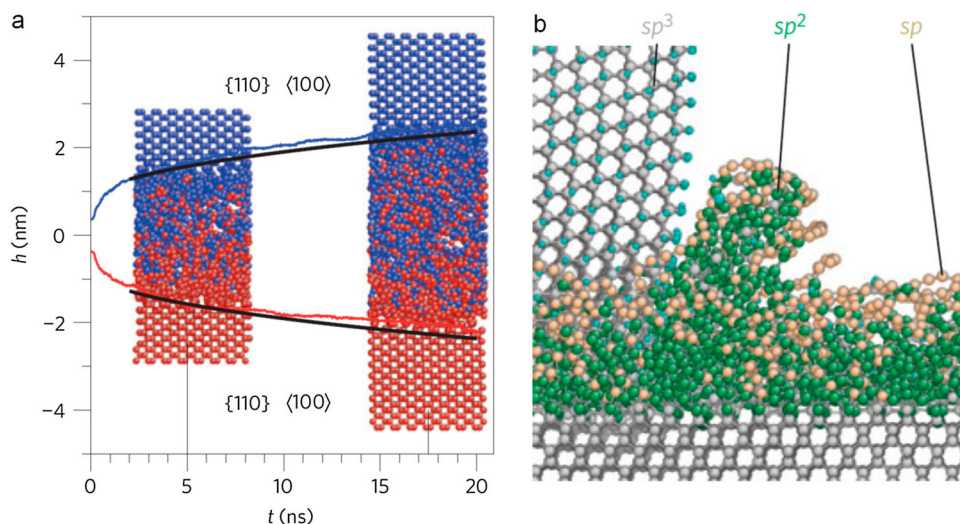
11   Molecular dynamics simulation of diamond polishing showing sp³-to-sp² transition. *a* The amorphous layer thickness increases with sliding. *b* Amorphous carbon accumulating at a diamond grit edge[188]

behave like a liquid with high mobility. In 1964 Pashley *et al.*[194] observed liquid-like behaviour in an *in situ* growth of gold and silver single crystal films in a TEM, where high surface diffusion led to coalescence of metal nuclei. Merkel and Marks[103] conducted *in situ* sliding test of gold nanofilm and recorded that a gold film can attach to a sliding tungsten probe at slightly elevated temperature of ~166°C. Figure 13*a* shows the TEM micrographs of a liquid-like gold neck connecting the probe and gold film. The gold neck region exhibited remarkable flexibility to accommodate deformation. Surface diffusion, which is ~300 nm²s⁻¹ for gold, was calculated to be equivalent to a viscosity of 1.61 Pa s at 166°C, about one order of magnitude greater than air. The temperature is significantly below the melting point of 1064°C, and thus bulk diffusion does not account for the high mobility.[103]

Liquid-like behaviour can significantly influence how the surfaces and wear debris interact with each other.

Lockwood *et al.*[195] exploited a NanoLAB TEM triboprobe[196] to rub a diamond probe on an FIB-machined aluminium alloy substrate without heating the specimen. The aluminium alloy specimen was heavily doped by gallium during the sample preparation. It is observed that the wear debris particles produced over time can behave like a liquid. Figure 13*b* shows two debris particle droplets on each side of the contacting surface.[195] Upon pushing the droplet, a liquid bridge was formed within 0.08 s. The meniscus on the side of the bridge revealed the liquid-like nature. EDS data showed that the droplets were mostly composed of gallium, and the liquid bridge resulted in complex capillary forces between the surfaces even when the surfaces were separated. Four-body (surfaces, wear debris and droplets) solid–liquid interactions need to been considered in this nano-scale sliding event. Atomistic simulation suggests that pseudoelastic deformation driven by surface diffusion can take place for <10 nm silver nanoparticles at room temperature.[197]
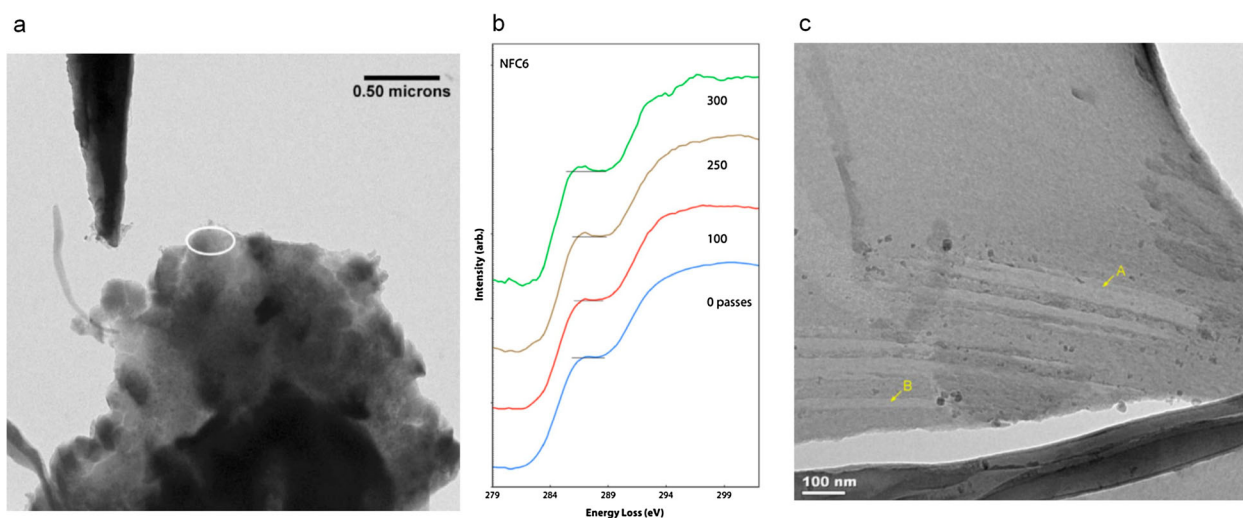
12   *a* TEM image of wear scar in DLC film after 300 sliding passes. The removal volume is estimated from the contrast of the groove.[104] *b* EELS spectrum of the DLC film showing increased sp² content after sliding.[104] *c* Sliding in wet N₂ produced significant wear in DCL film. The wear tracks are arrowed[109]
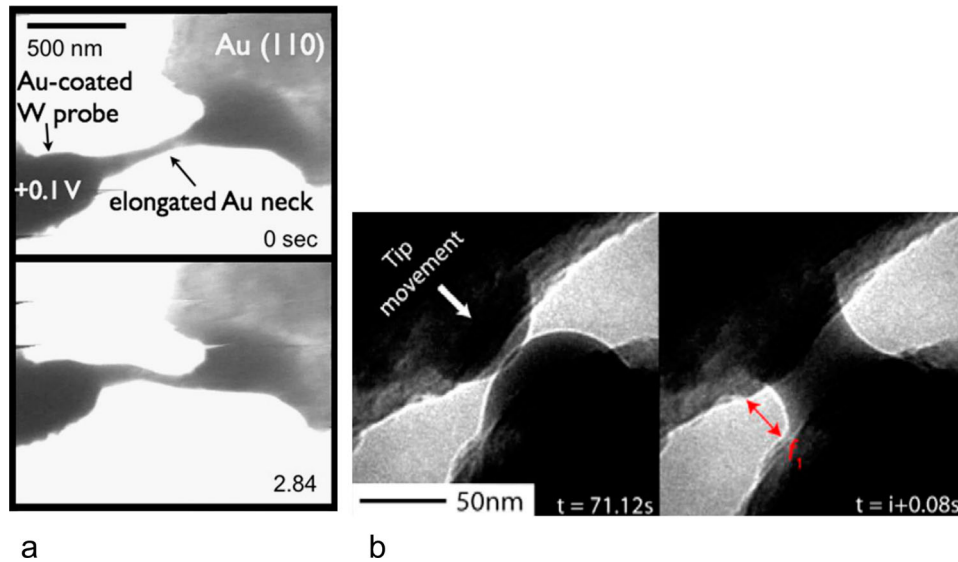
13 *a* A series of TEM micrograph show liquid-like behaviour of gold film *in situ* in a TEM. A highly plastically deformed gold bridged the tungsten probe and the gold film. The temperature of the contact is ~166°C due to small applied bias.[103] *b* Room-temperature liquid-like gallium forming a neck between two nano-droplets of doped gallium[195]

What do we know, what do not we know, whither the science

In situ TEM single asperity sliding experiments are still in their early stages. In some cases they have provided the first definitive proof of long established models in tribology; in a few cases they have demonstrated that new phenomena occur at the nanoscale, sometimes unexpected ones. In most cases they take place in electron microscopes which were not designed for this purpose with instruments where compromises have been made in the mechanical properties that can be measured and the accuracy of the tip/sample displacements. From a technical view these are exceedingly hard experiments to perform; we are aware of many more attempts to obtain useful tribological information than published papers which have had impact upon the field.

Rather than recapping what has been achieved, we will focus in this section on some reflective comments about what could be improved and where the field might progress in the future more as a perspective section. To date the image resolution reported is of low resolution around several nanometre during sliding. Most images and videos are based on mass contrast primarily due to lack of tilting capabilities in two dimensions and difficulties of preparing thin, defect-free sliding components. A dedicated imaging processing technique to filter out vibration and directional motion can be beneficial to improve image quality during sliding. Owing to electron beam damage, tribology of hydrocarbon-based polymeric materials, which play a significant role in various engineering applications, has not been investigated much in *in situ* TEM studies. A systematic study of reducing irradiation damage is required to understand organic materials sliding in *in situ* TEM tests. It may be that new low-voltage electron microscopes that are starting to become available have a promising further for this type of application.

From a tribological point of view, much work needs to be done for *in situ* TEM tribometers to simultaneously measure force and displacement in all three axes. In particular, the capability of lateral force measurement is extremely desired to acquire friction data of sliding interface. Most *in situ* TEM sliding to date has been performed in high vacuum, and thus may not fully represent what takes place in ambient atmosphere. With the state-of-the-art high-resolution and analytical TEM, it is desired to extend the full capability of advanced TEM to *in situ* TEM dynamic studies. In an aberration-corrected TEM, the gap between the poles of objective lens can be increased to accommodate a larger holder. Thus comprehensive analysis of atomic defects (such as dislocations) and surface atomic arrangement can be achieved at least in principle. In addition, *in situ* tribological tests in varied environment, such as gas, pressure, temperature and sliding speed, has become possible with the recent advance in environmental TEM.

Despite the aforementioned limitations current *in situ* TEM tribology investigations have provided unprecedented information on fundamental aspects of wear and friction at the nanometre scale. Conventional microscopic wear mechanisms usually involve materials plasticity and hardness, and in many cases can be extended to nanoscale sliding. Extensive plastic deformation, ploughing, chipping and third body rolling have been observed in great details in sliding single asperities. The dynamics of tribolayer formation and transfer have been recorded and related to the tribological behaviours at the macroscopic scale.[137–139,198]

Surfaces and nano-asperities can behave differently from their bulk form. The reports on liquid-like behaviour of gold film at sliding contact, thermally activated atomistic wear assisted by adhesion normal force, and steady wear of chromium carbide in a layer-by-layer fashion indicate that conventional wear mechanisms based on contact mechanics, adhesion and material plasticity may not fully account for single asperity wear at the nanometre scale. Much more work needs to be done in order to understand the breakdown of conventional continuum theories. Friction and wear are collective response of a

large number of atoms and defects at contact surface and sub-surface. Imaging the dynamics of these atoms will significantly extend our understanding of wear and friction at multiple length scales, such as atomic fracture due to friction or adhesion, defect initiation and evolution, tribofilm formation and transfer and chemical reactions with the environment and/or counterpart. The *in situ* TEM tribological tests have provided a unique tool to obtain direct experimental data for unravelling the mysteries.

In situ sliding in controlled environment, although with very limited access to, has begun to be investigated and the results are exploited to understand the sensitivity of a tribological process. The DLC film tested *in situ* in a TEM in dry condition was nearly wearless, and the presence of water vapour significantly accelerated wear loss. There is clear evidence that the tribological process can transform sp^2 carbon to sp^3 carbon with minimal thermal processes, and that the tribofilm played a critical role in the tribological process of DLC. By implementing cutting-edge analytical TEM tools, the influence of the environment can be resolving at the atomic scale.

Summary

Wear, lubrication and friction at the full length scales have received continuous attention. Dating back to the seminal work of Bowden and Tabor,[17,38] we know that solid–solid friction involves asperity-asperity contact at the micro to nanoscale. From a conventional materials science/mechanical properties approach, this is therefore going to involve both plastic and elastic processes. The process is of high complexity that requires comprehensive understanding of both materials intrinsic properties and extrinsic environmental. As recognised by Lucretius,[199] wear process involves small scale and was once beyond our power of observation. *In situ* tribological tests in a TEM have provided useful details of wear process of engineering materials at the nanoscale. With the integration of more sophisticated electron microscopy and tribometry techniques, more dramatic results on sliding interfaces will be anticipated in the future.

Acknowledgement

References

1. S. Bodman: 'The national academies summit on America's energy future', 2008, Washington, The National Academies of Sciences, Engineering, and Medicine.
2. H. P. Jost: 'The economic importance of tribology in the conservation of energy', in 'Tribologie Reibung Verschleiß Schmierung', (eds. W. Bunk *et al*.), 9–38; 1981, Berlin, Heidelberg, Springer.
3. B. Bhushan: 'Tribology: friction, wear, and lubrication', in 'The engineering handbook', (ed. R. C. Dorf), 2000, Boca Raton, FL, CRC Press LLC.
4. K. Holmberg, P. Andersson and A. Erdemir: 'Global energy consumption due to friction in passenger cars', *Tribol. Int.*, 2012, **47**, (0), 221–234.
5. D. Dowson: 'History of tribology', xxiv, 768; 1998, London, Professional Engineering Publishing.
6. H. P. Jost and G. B. M. o. Technology: 'Committee on tribology report, 1966–67', 1968, H.M. Stationery Office.
7. I. M. Hutchings: 'Tribology: friction and wear of engineering materials', 1992, London, Edward Arnold.
8. J. A. Williams: 'Engineering tribology', 1994, New York, Oxford University Press.
9. K. L. Johnson: 'Contact mechanics', 1985, Cambridge, Cambridge University Press.
10. B. Bhushan: 'Contact mechanics of rough surfaces in tribology: multiple asperity contact', *Tribol. Lett.*, 1998, **4**, (1), 1–35.
11. B. Bhushan: 'Handbook of micro/nanotribology', 628, [624] of plates; 1995, Boca Raton, CRC Press.
12. B. Bhushan and A. Majumdar: 'Fractal theory of the interfacial temperature distribution in the slow sliding regime .1. Elastic contact and heat-transfer analysis – discussion', *J Tribol-T Asme*, 1994, **116**, (4), 822.
13. J. F. Archard: 'Contact and rubbing of flat surfaces', *J. Appl. Phys.*, 1953, **24**, (8), 981–988.
14. K. L. Johnson: 'Mechanics of adhesion', *Tribol. Int.*, 1998, **31**, (8), 413–418.
15. D. Maugis: 'Adhesion of spheres: the JKR-DMT transition using a dugdale model', *J. Colloid Interface Sci.*, 1992, **150**, (1), 243–269.
16. B. V. Derjaguin, V. M. Muller and Y. P. Toporov: 'Effect of contact deformations on the adhesion of particles', *J. Colloid Interface Sci.*, 1975, **53**, (2), 314–326.
17. F. P. Bowden, A. J. W. Moore and D. Tabor: *J. Appl. Phys.*, 1942, **80**, 80–91.
18. Y. Liao, R. Pourzal, M. A. Wimmer, J. J. Jacobs, A. Fischer and L. D. Marks: 'Graphitic tribological layers in metal-on-metal hip replacements', *Science*, 2011, **334**, (6063), 1687–1690.
19. M. A. Wimmer, A. Fischer, R. Buscher, R. Pourzal, C. Sprecher, R. Hauert and J. J. Jacobs: *J. Orthop. Res.*, 2010, **28**, (4), 436–443.
20. L. D. Marks, O. L. Warren, A. M. Minor and A. P. Merkle: 'Tribology in full view', *MRS Bull.*, 2008, **33**, (12), 1168–1173.
21. M. A. Wimmer, C. Sprecher, R. Hauert, G. Tager and A. Fischer: 'Tribochemical reaction on metal-on-metal hip joint bearings', *Wear*, 2003, **255**, 1007–1014.
22. G. T. Gao, P. T. Mikulski and J. A. Harrison: 'Molecular-scale tribology of amorphous carbon coatings: effects of film thickness, adhesion, and long-range interactions', *J. Am. Chem. Soc.*, 2002, **124**, (24), 7202–7209.
23. M. A. Wimmer, J. Loos, R. Nassutt, M. Heitkemper and A. Fischer: 'The acting wear mechanisms on metal-on-metal hip joint bearings: in vitro results', *Wear*, 2001, **250**, 129–139.
24. A. Grill: 'Review of the tribology of diamond-like carbon', *Wear*, 1993, **168**, (1–2), 143–153.
25. R. S. Gates, S. M. Hsu and E. E. Klaus: 'Tribochemical mechanism of alumina with water', *Tribol. T.*, 1989, **32**, (3), 357–363.
26. Y. Yan, A. Neville and D. Dowson: 'Biotribocorrosion—an appraisal of the time dependence of wear and corrosion interactions: II. surface analysis', *J. Phys. D Appl. Phys.*, 2006, **39**, (15), 3206–3212.
27. C. A. Freyman, Y. F. Chen and Y. W. Chung: 'Synthesis of carbon films with ultra-low friction in dry and humid air', *Surf. Coat. Technol.*, 2006, **201**, (1–2), 164–167.
28. A. Erdemir: 'A crystal chemical approach to the formulation of self-lubricating nanocomposite coatings', *Surf. Coat. Technol.*, 2005, **200**, (5–6), 1792–1796.
29. J. Krim: 'Surface science and the atomic-scale origins of friction: what once was old is new again', *Surf. Sci.*, 2002, **500**, (1–3), 741–758.
30. J. M. Martin, T. Le Mogne, M. Boehm and C. Grossiord: 'Tribochemistry in the analytical UHV tribometer', *Tribol. Int.*, 1999, **32**, (11), 617–626.
31. R. W. Carpick and M. Salmeron: 'Scratching the surface: fundamental investigations of tribology with atomic force microscopy', *Chem. Rev.*, 1997, **97**, (4), 1163–1194.
32. A. P. Semenov: 'Tribology at high temperatures', *Tribol. Int.*, 1995, **28**, (1), 45–50.
33. J. M. Martin, T. Lemogne, C. Chassagnette and M. N. Gardos: 'Friction of hexagonal boron nitride in various environments', *Tribol. Trans.*, 1992, **35**, (3), 462–472.
34. B. Marchon, M. R. Khan, N. Heiman, P. Pereira and A. Lautie: 'Tribochemical wear on amorphous carbon thin films', *IEEE Trans. Magn.*, 1990, **26**, (5), 2670–2675.
35. B. Marchon, N. Heiman and M. R. Khan: 'Evidence for tribochemical wear on amorphous carbon thin films', *IEEE Trans. Magn.*, 1990, **26**, (1), 168–170.
36. F. P. Bowden, D. Tabor, N. Gane and R. F. Willis: 'Microdeformation of solids', *Z Phys. Chem-Leipzig*, 1970, **244**, (3–4), 129.
37. N. Gane and F. P. Bowden: 'Microdeformation of solids', *J. Appl. Phys.*, 1968, **39**, (3), 1432–1436.
38. F. P. Bowden and D. Tabor: 'The friction and lubrication of solids', 1950, Oxford, Clarendon Press.

39. R. Maboudian and C. Carraro: 'Surface chemistry and tribology of MEMS', *Annu. Rev. Phys. Chem.*, 2004, **55**, 35–54.

40. N. R. Tas, C. Gui and M. Elwenspoek: 'Static friction in elastic adhesion contacts in MEMS', *J. Adhes. Sci. Technol.*, 2003, **17**, 547–561.

41. D. A. Rigney: 'Comments on the sliding wear of metals', *Tribol. Int.*, 1997, **30**, (5), 361–367.

42. R. Bennewitz, E. Gnecco, T. Gyalog and E. Meyer: 'Atomic friction studies on well-defined surfaces', *Tribol. Lett.*, 2001, **10**, (1–2), 51–56.

43. B. Bhushan: 'Nanoscale tribophysics and tribomechanics', *Wear*, 1999, **225-229**, (Part 1), 465–492.

44. R. W. Carpick, N. Agrait, D. F. Ogletree and M. Salmeron: 'Measurement of interfacial shear (friction) with an ultrahigh vacuum atomic force microscope', *J. Vac. Sci. Technol. B Microelectron. Nanometer Struct.*, 1996, AVS, 1289–1295.

45. D. Marchetto, A. Rota, L. Calabri, G. C. Gazzadi, C. Menozzi and S. Valeri: 'AFM investigation of tribological properties of nano-patterned silicon surface', *Wear*, 2008, **265**, (5–6), 577–582.

46. R. G. Miller and P. J. Bryant: 'Atomic force microscopy of layered compounds', *J. Vac. Sci. Technol. A*, 1989, **7**, (4), 2879–2881.

47. J.-A. Ruan and B. Bhushan: 'Atomic-scale and microscale friction studies of graphite and diamond using friction force microscopy', *J. Appl. Phys.*, 1994, **76**, (9), 5022–5035.

48. I. L. Singer, H. M. Pollock and North Atlantic Treaty Organization. Scientific Affairs Division: 'Fundamentals of friction: macroscopic and microscopic processes', xv, 621; 1992, Dordrecht, Boston, Kluwer Academic.

49. H. I. Kim and J. R. Lince: 'Direct visualization of sliding-induced tribofilm on Au/MoS2 nanocomposite coatings by c-AFM', *Tribol. Lett.*, 2007, **26**, (1), 61–65.

50. I. Heyvaert, J. Krim, C. VanHaesendonck and Y. Bruynseraede: 'Surface morphology and kinetic roughening of Ag on Ag(111) studied with scanning tunneling microscopy', *Phys. Rev. E*, 1996, **54**, (1), 349–353.

51. M. Hirano, K. Shinjo, R. Kaneko and Y. Murata: 'Observation of superlubricity by scanning tunneling microscopy', *Phys. Rev. Lett.*, 1997, **78**, (8), 1448–1451.

52. M. Iwatsuki, K. Murooka, S. Kitamura, K. Takayanagi and Y. Harada: *J. Electron Microsc.*, 1991, **40**, (1), 48–53.

53. G. Palasantzas and J. Krim: 'Scanning tunneling microscopy study of the thick film limit of kinetic roughening', *Phys. Rev. Lett.*, 1994, **73**, (26), 3564–3567.

54. J. C. H. Spence: 'A scanning tunneling microscope in a side-entry holder for reflection electron microscopy in the philips EM400', *Ultramicroscopy*, 1988, **25**, (2), 165–169.

55. E. W. van der Vegte and G. Hadziioannou: 'Scanning force microscopy with chemical specificity: an extensive study of chemically specific tip–surface interactions and the chemical imaging of surface functional groups', *Langmuir*, 1997, **13**, (16), 4357–4368.

56. H. Ohnishi, Y. Kondo and K. Takayanagi: 'UHV electron microscope and simultaneous STM observation of gold stepped surfaces', *Surf. Sci.*, 1998, **415**, (3), L1061–L1064.

57. F. J. Giessibl, M. Herz and J. Mannhart: 'Friction traced to the single atom', *PNAS*, 2002, **99**, (19), 12006–12010.

58. G. Stachowiak and A. W. Batchelor: 'Engineering tribology', 2013, Oxford, Butterworth-Heinemann.

59. J. F. Archard: 'Single contacts and multiple encounters', *J. Appl. Phys.*, 1961, **32**, 1420–1425.

60. D. A. Rigney, R. Divakar and S. M. Kuo: 'Deformation substructures associated with very large plastic strains', *Scripta Metall. Mater.*, 1992, **27**, 975–980.

61. S. Johansson and J. Schweitz: 'Contact damage in single-crystalline silicon investigated by cross-sectional transmission electron microscopy', *J. Am. Ceram. Soc.*, 1988, **71**, 617–623.

62. J. C. Morris and D. L. DCallahan: 'Origins of microplasticity in low-load scratching of silicon', *J. Mater. Res.*, 1994, **9**, (11), 2907–2913.

63. R. Stickler and G. R. Booker: 'Surface damage on abraded silicon specimens', *Philos. Mag. A*, 1963, **8**, (89), 859–876.

64. K. E. Puttick, L. C. Whitmore, C. L. Chao and A. E. Gee: 'Transmission electron microscopy of nanomachined silicon crystals', *Philos. Mag.*, 1994, **69**, 91–103.

65. D. A. Rigney, M. G. S. Naylor, R. Divakar and L. K. Ives: 'Low energy dislocation structures caused by sliding and by particle impact', *Mater. Sci. Eng.*, 1986, **81**, 409–425.

66. J. Don and D. A. Rigney: 'Prediction of debris flake thickness', *Wear*, 1985, **105**, (1), 63–72.

67. P. Heilmann and D. A. Rigney: 'An energy-based model of friction and its application to coated systems', *Wear*, 1981, **72**, (2), 195–217.

68. I. A. Polonsky and L. M. Keer: 'Scale effects of elastic-plastic behavior of microscopic asperity contacts', *J. Tribol.*, 1996, **118**, (2), 335–340.

69. D. A. Rigney: 'Transfer, mixing and associated chemical and mechanical processes during the sliding of ductile materials', *Wear*, 2000, **245**, (1–2), 1–9.

70. D. Tabor: 'Friction: the present state of our understanding', *J. Lubr. Technol.*, 1981, **103**, (2), 169–179.

71. S. C. Lim and M. F. Ashby: 'Overview no. 55 wear-mechanism maps', *Acta Metall.*, 1987, **35**, (1), 1–24.

72. D. A. Rigney: 'Sliding wear of metals', *Annu. Rev. Mater. Sci.*, 1988, **18**, 141–163.

73. N. Gane: 'The direct measurement of the strength of metals on a sub-micrometre scale', *Proc. Math. Phys. Eng. Sci.*, 1970, **317**, 367–391.

74. K. Kato, T. Kayaba, Y. Endo and K. Hokkirigawa: 'Three dimensional shape effect on abrasive Wear', *J. Tribol.*, 1986, **108**, (3), 346–349.

75. K. Hokkirigawa, K. Kato and Z. Z. Li: 'The effect of hardness on the transition of the abrasive wear mechanism of steels', *Wear*, 1988, **123**, (2), 241–251.

76. K. Hokkirigawa and K. Kato: 'An experimental and theoretical investigation of ploughing, cutting and wedge formation during abrasive wear', *Tribol. Int.*, 1988, **21**, (1), 51–57.

77. H. Kitsunai, K. Kato, K. Hokkirigawa and H. Inoue: 'The transitions between microscopic wear modes during repeated sliding friction observed by a scanning electron microscope tribosystem', *Wear*, 1990, **135**, 237–249.

78. H. Kitsunai, K. Hokkirigawa, N. Tsumaki and K. Kato: 'Transitions of microscopic wear mechanism for Cr_2O_3 ceramic coatings during repeated sliding observed in a scanning électron microscope tribosystem', *Wear*, 1991, **151**, (2), 279–289.

79. H. Kitsunai and K. Hokkirigawa: 'Transitions of microscopic wear mode of silicon carbide coatings by chemical vapor deposition during repeated sliding observed in a scanning electron microscope tribosystem', *Wear*, 1995, **185**, (1–2), 9–15.

80. P. B. Hirsch: 'Electron microscopy of thin crystals', 1977, Huntington, NY, R.E. Krieger Pub. Co.

81. J. C. H. Spence: 'High-resolution electron microscopy', 2013, London, Oxford University Press.

82. L. M. Peng, S. L. Dudarev and M. J. Whelan: 'High-energy electron diffraction and microscopy', 2011, Oxford University Press.

83. J. M. Cowley: 'Diffraction physics', 1995, New York, Elsevier Science Ltd.

84. L. Reimer and H. Kohl: 'Transmission electron microscopy: physics of image formation', 2008, New York, Springer.

85. Hysitron. 2015. 'TEM PicoIndenter', [Available from: https://www.hysitron.com/.

86. A. M'ndange-Pfupfu, O. Eryilmaz, A. Erdemir and L. Marks: 'Quantification of sliding-induced phase transformation in N3FC diamond-like carbon films', *Diam. Relat. Mater.*, 2011, **20**, 1143–1148.

87. A. P. Merkle: 'Tribological interfaces studied by an analytical dislocation model and in-situ transmission electron microscopy', PhD thesis, Northwestern University, Evanston, IL, 2007.

88. M. Kuwabara, W. Lo and J. C. H. Spence: 'Reflection electron microscope imaging of an operating scanning tunneling microscope', *J. Vac. Sci. Technol. A*, 1989, **7**, 2745–2751.

89. W. K. Lo and J. C. H. Spence: 'Investigation of STM image artifacts by in-situ reflection electron microscopy', *Ultramicroscopy*, 1993, **48**, 433–444.

90. J. C. H. Spence, W. Lo and M. Kuwabara: 'Observation of the graphite surface by reflection electron microscopy during STM operation', *Ultramicroscopy*, 1990, **33**, 69–82.

91. T. Sato, T. Ishida, S. Nabeya and H. Fujita: 'Nano-scale observation of frictional deformation at Ag single point contact with MEMS-in-TEM setup', *J. Phys. Conf. Ser.*, 2010, **258**, 012005.

92. M. W. Larsson, L. R. Wallenberg, A. I. Persson and L. Samuelson: 'Probing of individual semiconductor nanowhiskers by TEM-STM', *Microsc. Microanal.*, 2004, **10**, (1), 41–46.

93. K. Anantheshwara and M. S. Bobji: *Tribol. Int.*, 2010, **43**, (5–6), 1099–1103.

94. K. Svensson, Y. Jompol, H. Olin and E. Olsson: 'Compact design of a transmission electron microscope-scanning tunneling microscope holder with three-dimensional coarse motion', *Rev. Sci. Instrum.*, 2003, **74**, (11), 4945–4947.

95. Y. Oshima, K. Mouri, H. Hirayama and K. Takayanagi: *Surf. Sci.*, 2003, **531**, (3), 209–216.

96. H. Nili, K. Kalantar-zadeh, M. Bhaskaran and S. Sriram: 'In situ nanoindentation: probing nanoscale multifunctionality', *Prog. Mater. Sci.*, 2013, **58**, (1), 1–29.

97. D. Erts, A. Lohmus, R. Lohmus, H. Olin, A. V. Pokropivny, L. Ryen and K. Svensson: 'Force interactions and adhesion of gold contacts using a combined atomic force microscope and transmission electron microscope', *Appl. Surf. Sci.*, 2002, **188**, 460–466.

98. M. A. Wall and U. Dahmen: 'An in situ nanoindentation specimen holder for a high voltage transmission electron microscope', *Microsc. Res. Tech.*, 1998, **42**, (4), 248–254.

99. M. S. Bobji, C. S. Ramanujan, R. C. Doole, J. B. Pethica and B. J. Inkson: 'An in-situ TEM nanoindenter system with 3-axis inertial positioner', *Mater. Res. Soc. Symp. Proc.*, 2003, **778**, 105–110.

100. T. Kizuka, K. Yamada, S. Deguchi, M. Naruse and N. Tanaka: 'Cross-sectional time-resolved high-resolution transmission electron microscopy of atomic-scale contact and noncontact-type scannings on gold surfaces', *Phys. Rev. B*, 1997, **55**, (12), R7398–R7401.

101. A. Nafari, D. Karlen, C. Rusu, K. Svensson, H. Olin and P. Enoksson: 'MEMS sensor for in situ TEM atomic force Microscopy', *J. Microelectromech. S*, 2008, **17**, (2), 328–333.

102. T. Sato, T. Ishida, L. Jalabert and H. Fujita: 'Real-time transmission electron microscope observation of nanofriction at a single Ag asperity', *Nanotechnology*, 2012, **23**, 505701.

103. A. P. Merkle and L. D. Marks: 'Liquid-like tribology of gold studied by in situ TEM', *Wear*, 2008, **265**, (11–12), 1864–1869.

104. A. P. Merkle, A. Erdemir, O. L. Eryilmaz, J. A. Johnson and L. D. Marks: 'In situ TEM studies of tribo-induced bonding modifications in near-frictionless carbon films', *Carbon*, 2010, **48**, (3), 587–591.

105. Y. Liao, E. Hoffman and L. D. Marks: 'Nanoscale abrasive wear of coCrMo in in situ TEM sliding', *Tribol. Lett.*, 2015, **57**, 3.

106. A. P. Merkle and L. D. Marks: 'Friction in full view', *Appl. Phys. Lett.*, 2007, **90**, (6), 064101.

107. C. A. Volkert and A. M. Minor: 'Focused ion beam microscopy and micromachining', *MRS Bull.*, 2007, **32**, (5), 389–399.

108. O. L. Warren, Z. W. Shan, S. A. S. Asif, E. A. Stach, J. W. Morris and A. M. Minor: 'In situ nanoindentation in the TEM', *Mater. Today*, 2007, **10**, (4), 59–60.

109. A. M'ndange-Pfupfu, J. Ciston, O. Eryilmaz, A. Erdemir and L. D. Marks: 'Direct observation of tribochemically assisted wear on diamond-like carbon thin Films', *Tribol. Lett.*, 2013, **49**, (2), 351–356.

110. J. R. Yang, Z. Liu, F. Grey, Z. P. Xu, X. D. Li, Y. L. Liu, M. Urbakh, Y. Cheng and Q. S. Zheng: 'Observation of high-speed microscale superlubricity in graphite', *Phys. Rev. Lett.*, 2013, **110**, (25), 255504.

111. T. W. Scharf and S. V. Prasad: 'Solid lubricants: a review', *J. Mater. Sci.*, 2013, **48**, (2), 511–531.

112. I. Leven, D. Krepel, O. Shemesh and O. Hod: 'Robust superlubricity in graphene/h-BN heterojunctions', *J. Phys. Chem. Lett.*, 2013, **4**, (1), 115–120.

113. A. S. de Wijn, C. Fusco and A. Fasolino: 'Stability of superlubric sliding on graphite', *Phys. Rev. E*, 2010, **81**, (4), 046105.

114. J. J. Hu, R. Wheeler, J. S. Zabinski, P. A. Shade, A. Shiveley and A. A. Voevodin: 'Transmission electron microscopy analysis of Mo–W–S–Se film sliding contact obtained by using focused ion beam microscope and in situ microtribometer', *Tribol. Lett.*, 2008, **32**, (1), 49–57.

115. J. Cumings and A. Zettl: 'Low-friction nanoscale linear bearing realized from multiwall carbon nanotubes', *Science*, 2000, **289**, (5479), 602–604.

116. M. Chhowalla and G. A. J. Amaratunga: 'Thin films of fullerene-like MoS_2 nanoparticles with ultra-low friction and wear', *Nature*, 2000, **407**, (6801), 164–167.

117. C. M. Mate, G. M. McClelland, R. Erlandsson and S. Chiang: 'Atomic-scale friction of a tungsten tip on a graphite surface', *Phys. Rev. Lett.*, 1987, **59**, (17), 1942–1945.

118. J. Krim, J. P. Coulomb and J. Bouzidi: 'Summary abstract: influence of film melting characteristics on the wetting behavior of multilayer oxygen films adsorbed on graphite', *J. Vac. Sci. Technol. A*, 1987, **5**, (4), 1096–1097.

119. J. Skinner, N. Gane and D. Tabor: 'Micro-friction of graphite', *Nat. Phys. Sci.*, 1971, **232**, (35), 195–196.

120. R. H. Savage: 'Graphite lubrication', *J. Appl. Phys.*, 1948, **19**, (1), 1–10.

121. U. D. Schwarz, O. Zworner, P. Koster and R. Wiesendanger: 'Quantitative analysis of the frictional properties of solid materials at low loads. I. carbon compounds', *Phys. Rev. B*, 1997, **56**, 6987–6996.

122. M. Dienwiebel, G. S. SVerhoeven, N. Pradeep and J. W. M. Frenken: 'Superlubricity of graphite', *Phys. Rev. Lett.*, 2004, **92**, (12), 126101–126104.

123. G. Casillas, Y. Liao, M. Jose-Yacaman and L. D. Marks: 'Monolayer transfer layers during sliding at the atomic scale', *Tribol. Lett.*, 2015, **59**, (3), 1–5.

124. J. Luo, H. D. Jang, T. Sun, L. Xiao, Z. He, A. Katsoulidis, M. Kanatzidis, J. M. Gibson and J. X. Huang: 'Compression and aggregation-resistant particles of crumpled soft sheets', *ACS Nano*, 2011, **5**, 8943–8949.

125. D. Tang, D. G. Kvashnin, S. Najmaei, Y. Bando, K. Kimoto, P. Koshinen, P. M. Ajayan, B. I. Yakobson, P. B. Sorokin, J. Lou and D. Golberg: 'Holocene variations in peatland methane cycling associated with the asian summer monsoon system', *Nat. Commun.*, 2014, **5**, 4631–4638.

126. J. P. Oviedo, S. KC, N. Lu, J. Wang, K. Cho, R. M. Wallace and M. J. Kim: 'In situ TEM characterization of shear-stress-induced interlayer sliding in the cross section view of molybdenum disulfide', *ACS Nano*, 2015, **9**, (2), 1543–1551.

127. I. L. Singer, R. N. Bolster, J. Wegand, S. Fayeulle and B. C. Stupp: 'Hertzian stress contribution to low friction behavior of thin MoS_2 coatings', *Appl. Phys. Lett.*, 1990, **57**, 995–997.

128. L. Rapoport, Y. Bilik, Y. Feldman, M. Homyonfer, S. R. Cohen and R. Tenne: 'Hollow nanoparticles of WS_2 as potential solid-state lubricants', *Nat. Commun.*, 1997, **387**, 791–793.

129. L. Rapoport, Y. Feldman, M. Homyonfer, H. Cohen, J. Sloan, J. L. Hutchison and R. Tenne: 'Inorganic fullerene-like material as additives to lubricants: structure-function relationship', *Wear*, 1999, **975**, 225–229.

130. L. Cizaire, B. Vacher, T. Le Mogne, J. M. Martin, L. Rapoport, A. Margolin and R. Tenne: 'Mechanisms of ultra-low friction by hollow inorganic fullerene-like MoS_2 nanoparticles', *Surf. Coat. Tech.*, 2002, **160**, 282–287.

131. R. Rosentsveig, A. Gorodnev, N. Feuerstein, H. Friedman, A. Zak, N. Fleischer, J. Tannous, F. Dassenoy and R. Tenne: 'Fullerene-like MoS_2 nanoparticles and their tribological behavior', *Tribol. Lett.*, 2009, **36**, 175–182.

132. L. Joly-Pottuz, J. M. Martin, F. Dassenoy, M. Belin, R. Montagnac and B. Reynard: 'Pressure-induced exfoliation of inorganic fullerene-like WS_2 particles in a hertzian contact', *J. Appl. Phys.*, 2006, **99**, 023524–023526.

133. I. Lahouij, F. Dassenoy, L. Knoop, J. M. Martin and B. Vacher: 'In situ TEM observation of the behavior of an individual fullerene-like MoS_2 nanoparticle in a dynamic contact', *Tribol. Lett.*, 2011, **42**, 133–140.

134. J. Ruan and B. Bhushan: 'Nanoindentation studies of sublimed fullerene films using atomic force microscopy', *J. Mater. Res.*, 1993, **8**, (12), 3019–3022.

135. M. Godet: 'The third-body approach: a mechanical view of wear', *Wear*, 1984, **100**, 437–452.

136. I. L. Singer, S. Fayeulle and P. D. Ehni: 'Friction and wear behavior of TiN in air: the chemistry of transfer films and debris formation', *Wear*, 1991, **149**, (1–2), 375–394.

137. T. W. Scharf and I. L. Singer: 'Role of the transfer film on the friction and wear of metal carbide reinforced amorphous carbon coatings during run-in', *Tribol. Lett.*, 2009, **36**, (1), 43–53.

138. T. W. Scharf and I. L. Singer: 'Monitoring transfer films and friction instabilities with in situ Raman tribometry', *Tribol. Lett.*, 2003, **14**, (1), 3–8.

139. T. W. Scharf and I. L. Singer: 'Quantification of the thickness of carbon transfer films using Raman tribometry', *Tribol. Lett.*, 2003, **14**, (2), 137–145.

140. T. W. Scharf, P. G. Kotula and S. V. Prasad: 'Friction and wear mechanisms in MoS_2/Sb2O$_3$/Au nanocomposite coatings', *Acta Mater.*, 2010, **58**, 4100–4109.

141. K. J. Wahl, D. N. Dunn and I. L. Singer: 'Wear behavior of Pb–Mo–S solid lubricating coatings', *Wear*, 1999, **230**, (2), 175–183.

142. C. B. Rieker, R. Schon and P. Kottig: *J. Arthroplasty*, 2004, **19**, (8), 5–11.

143. S. A. Jacobsson, K. Djerf and O. Wahlstrom: '20-year results of mcKee-farrar versus charnley prosthesis', *Clin. Orthop. Relat. Res.*, 1996, **329**, S60–S68.

144. L. D. Dorr, Z. I. Wang, D. B. Longjohn, B. Dubois and R. Murken: *J. Bone Joint Surg. Am.*, 2000, **82A**, (6), 789–798.

145. C. P. Delaunay, F. Bonnomet, P. Clavert, P. Laffargue and H. Migaud: 'THA using metal-on-metal articulation in active patients younger than 50 years', *Clin. Orthop. Relat. Res.*, 2008, **466**, (2), 340–346.

146. V. Eswaramoorthy, P. Moonot, Y. Kalairajah, L. C. Biant and R. E. Field: 'The metasul metal-on-metal articulation in primary

total hip replacement: clinical and radiological results at ten years', *J. Bone Joint Surg. Br.*, 2008, **90-B**, (10), 1278–1283.

147. D. Dowson, C. M. McNie and A. A. J. Goldsmith: 'Direct experimental evidence of lubrication in a metal-on-metal total hip replacement tested in a joint simulator', *Proc. Inst. Mech. Eng. C J Mech. Eng. Sci.*, 2000, **214**, (1), 75–86.

148. D. Sun, J. A. Wharton, R. J. K. Wood, L. Ma and W. M. Rainforth: 'Microabrasion–corrosion of cast coCrMo alloy in simulated body fluids', *Tribol. Int.*, 2009, **42**, (1), 99–110.

149. Y. Liao, R. Pourzal, P. Stemmer, M. A. Wimmer, J. J. Jacobs, A. Fischer and L. Marks: 'New insights into hard phases of coCrMo metal-on-metal hip replacements', *J. Mech. Behav. Biomed. Mater.*, 2012, **12**, 39–49.

150. H. F. Lopez and A. J. Saldivar-Garcia: 'Martensitic transformation in a cast Co-Cr-Mo-C alloy', *Metall. Mater. Trans. A*, 2008, **39**, (1), 8–18.

151. K. Asgar and F. A. Peyton: 'Effect of microstructure on the physical properties of cobalt-base alloys', *J. Dent. Res.*, 1961, **40**, (1), 63–72.

152. M. J. Murray, P. J. Mutton and J. D. Watson: 'Abrasive wear mechanisms in steels', *J. Lubr. Technol.*, 1982, **104**, (1), 9–16.

153. J. M. Challen and P. L. B. Oxley: 'An explanation of the different regimes of friction and wear using asperity deformation models', *Wear*, 1979, **53**, (2), 229–243.

154. J. M. Challen, P. L. B. Oxley and E. D. Doyle: 'The effect of strain hardening on the critical angle for abrasive (chip formation) wear', *Wear*, 1983, **88**, (1), 1–12.

155. K. Kato: 'Micro-mechanisms of wear — wear modes', *Wear*, 1992, **153**, (1), 277–295.

156. K. L. Johnson: 'Contact mechanics and the wear of metals', *Wear*, 1995, **190**, (2), 162–170.

157. E. D. Doyle and L. E. Samuels: 'Further development of a model of grinding', *Proc. Int. Conf. Prod. Eng.*, 1974, **2**, 45–50.

158. K. Anantheshwara, K. A. Selvan, R. K. Mishra and M. S. Bobji: 'In situ transmission electron microscopy study of deformation of an aluminum alloy tribolayer', *Scripta. Mater.*, 2009, **60**, 623–626.

159. R. Buscher, G. Tager, W. Dudzinski, B. Gleising, M. A. Wimmer and A. Fischer: 'Subsurface microstructure of metal-on-metal hip joints and its relationship to wear particle generation', *J. Biomed. Mater. Res. B Appl. Biomater.*, 2005, **72B**, (1), 206–214.

160. R. Buscher and A. Fischer: 'The pathways of dynamic recrystallization in all-metal hip joints', *Wear*, 2005, **259**, 887–897.

161. M. Bryant, M. Ward, R. Farrar, R. Freeman, K. Brummitt, J. Nolan and A. Neville: 'Characterisation of the surface topography, tomography and chemistry of fretting corrosion product found on retrieved polished femoral stems', *J. Mech. Behav. Biomed. Mater.*, 2014, **32**, 321–334.

162. T. D. B. Jacobs, B. Gotsmann, M. A. Lantz and R. W. Carpick: 'On the application of transition state theory to atomic-scale wear', *Tribol. Lett.*, 2010, **39**, (3), 257–271.

163. N. P. Suh: 'An overview of the delamination theory of wear', *Wear*, 1977, **44**, (1), 1–16.

164. T. D. B. Jacobs and R. W. Carpick: 'Nanoscale wear as a stress-assisted chemical reaction', *Nat. Nanotechnol.*, 2013, **8**, (2), 108–112.

165. B. Gotsmann and M. A. Lantz: 'Atomistic wear in a single asperity sliding contact', *Phys. Rev. Lett.*, 2008, **101**, (12), 125501.

166. H. Bhaskaran, B. Gotsmann, A. Sebastian, U. Drechsler, M. A. Lantz, M. Despont, P. Jaroenapibal, R. W. Carpick, Y. Chen and K. Sridharan: 'Ultralow nanoscale wear through atom-by-atom attrition in silicon-containing diamond-like carbon', *Nat. Nanotechnol.*, 2010, **5**, (3), 181–185.

167. P. Steiner, E. Genecco, F. Krok, J. Budzioch, L. Walczk, J. Konior, M. Szymonski and E. Meyer: 'Atomic-scale friciton on stepped surfaces of ionic crystals', *Phys. Rev. Lett.*, 2001, **106**, 186101–186104.

168. E. Gnecco, R. Bennewitz and E. Meyer: 'Abrasive wear on the atomic scale', *Phys. Rev. Lett.*, 2002, **88**, (21), 215501.

169. A. R. Konicek, D. S. Grierson, P. U. P. A. Gilbert, W. G. Sawyer, A. V. Sumant and R. W. Carpick: 'Origin of ultralow friction and wear in ultrananocrystalline diamond', *Phys. Rev. Lett.*, 2008, **100**, 235501–235503.

170. D. Hannouche, M. Hamadouche, R. Nizard, P. Bizot, A. Meunier and L. Sedel: 'Ceramics in total hip replacement', *Clin. Orthop. Relat. Res.*, 2005, **430**, 62–71.

171. K. Kato and K. Adachi: 'Wear of advanced ceramics', *Wear*, 2002, **253**, (11–12), 1097–1104.

172. Y. Liao and L. D. Marks: 'Direct observation of layer-by-layer wear', *Tribol. Lett.*, 2015, **59**, (3), 1–11.

173. A. L. Bowman, G. P. Arnold, E. K. Storms and N. G. Nereson: 'The crystal structure of $Cr_{23}C_6$', *Acta Crystallogr. Sec B*, 1972, **28**, (10), 3102–3103.

174. M. El-Batanouny, S. Burdick, K. M. Martini and P. Stancioff: 'Double-sine-Gordon solitons: a model for misfit dislocations on the Au(111) reconstructed surface', *Phys. Rev. Lett.*, 1987, **58**, (26), 2762–2765.

175. F. Ernst: 'Dissociation of misfit dislocation nodes in (111) Gesi/Si interfaces', *Philos. Mag. A-Phys.*, 1993, **68**, (6), 1251–1272.

176. F. C. Frank and J. H. v. d. Merwe: 'One-dimensional dislocations. II. misfitting monolayers and oriented overgrowth', *Proc. Math. Phys. Eng. Sci.*, 1949, **198**, (1053), 216–225.

177. R. Kohler, J.-U. Pfeiffer, H. Raidt, W. Neumann, P. Zaumseil and U. Richter: 'Nucleation, glide velocity and blocking of misfit dislocations in siGe/Si', *Cryst. Res. Technol.*, 1998, **33**, (4), 593–604.

178. T. Schober and R. W. Balluffi: 'Quantitative observation of misfit dislocation arrays in low and high angle twist grain boundaries', *Philos. Mag.*, 1970, **21**, (169), 109.

179. L. E. Shilkrot and D. J. Srolovitz: 'Elastic analysis of finite stiffness bimaterial interfaces: application to dislocation–interface interactions', *Acta Mater.*, 1998, **46**, (9), 3063–3075.

180. W. Mader and D. Knauss: 'Equilibrium position of misfit dislocations at planar interfaces', *Acta Metallurgica Et Materialia*, 1992, **40**, S207–S215.

181. F. P. Bowden: 'Introduction to the discussion: the mechanism of friction', *Proc. Math. Phys. Eng. Sci.*, 1952, **212**, (1111), 440–449.

182. F. P. Bowden and E. H. Freitag: 'The friction of solids at very high speeds. I. metal on metal; II. metal on diamond', *Proc. Math. Phys. Eng. Sci.*, 1958, **248**, (1254), 350–367.

183. A. P. Merkle and L. D. Marks: 'A predictive analytical friction model from basic theories of interfaces, contacts and dislocations', *Tribol. Lett.*, 2007, **26**, (1), 73–84.

184. A. M'ndange-Pfupfu and L. D. Marks: 'A dislocation-based analytical model for the nanoscale processes of shear and plowing friction', *Tribol. Lett.*, 2010, **39**, 163.

185. J. de la Figuera, K. Pohl, O. R. de la Fuente, A. K. Schmid, N. C. Bartelt, C. B. Carter and R. Q. Hwang: 'Direct observation of misfit dislocation glide on surfaces', *Phys. Rev. Lett.*, 2001, **86**, (17), 3819–3822.

186. K. Anantheshwara, A. J. Lockwood, R. K. Mishra, B. Inkson and M. S. Bobji: 'Dynamical evolution of wear particles in nanocontacts', *Tribol. Lett.*, 2012, **45**, 229–235.

187. A. Erdemir and C. Donnet: 'Tribology of diamond-like carbon films: recent progress and future prospects', *J. Phys. D Appl. Phys.*, 2006, **39**, R311–R327.

188. L. Pastewka, S. Moser, P. Gumbsch and M. Moseler: 'Anisotropic mechanical amorphization drives wear in diamond', *Nat. Mater.*, 2011, **10**, (1), 34–38.

189. C. Donnet, T. L. Mogne, L. Ponsonnet, M. Belin, A. Grill, V. Patel and C. Jahnes: 'The respective role of oxygen and water vapor on the tribology of hydrogenated diamond-like carbon coatings', *Tribol. Lett.*, 1998, **4**, (3–4), 259–265.

190. A. Erdemir: 'The role of hydrogen in tribological properties of diamond-like carbon films', *Surf. Coat. Technol.*, 2001, **146–147**, 292–297.

191. A. Grill: 'Tribology of diamond like carbon and related materials: an updated review', *Surf. Coat. Technol.*, 1997, **94–95**, (1–3), 507–513.

192. F. M. Borodich and L. M. Keer: 'Modeling effects of gas adsorption and removal on friction during sliding along diamond-like carbon films', *Thin Solid Films*, 2005, **476**, (1), 108–117.

193. A. Erdemir: 'Review of engineered tribological interfaces for improved boundary lubrication', *Tribol. Int.*, 2005, **38**, (3), 249–256.

194. D. W. Pashley, M. J. Stowell, M. H. Jacobs and T. J. Law: 'The growth and structure of gold and silver deposits formed by evaporation inside an electron microscope', *Philos. Mag.*, 1964, **10**, (103), 127–158.

195. A. J. Lockwood, K. Anantheshwara, M. S. Bobji and B. Inkson: 'Friction-formed liquid droplets', *Nanotechnology*, 2011, **22**, 105703 .

196. J. J. Wang, A. J. Lockwood, Y. Peng, X. Xu, M. S. Bobji and B. J. Inkson: *Nanotechnology*, 2009, **20**, (30), 305–703.

197. J. Sun, L. He, Y. C. Lo, H. Bi, L. Sun, Z. Zhang, S. X. Mao and J. Li: 'Liquid-like pseudoelasticity of sub-10-nm crystalline silver particles', *Nat. Mater.*, 2014, **13**, 1007–1012.

198. T. W. Scharf and I. L. Singer: 'Thickness of diamond-like carbon coatings quantified with Raman spectroscopy', *Thin Solid Films*, 2003, **440**, (1–2), 138–144.

199. T. Lucretius Carus and A. E. Stallings: 'De rerum natura (On the nature of things)', 2007, London, Penguin Classics.